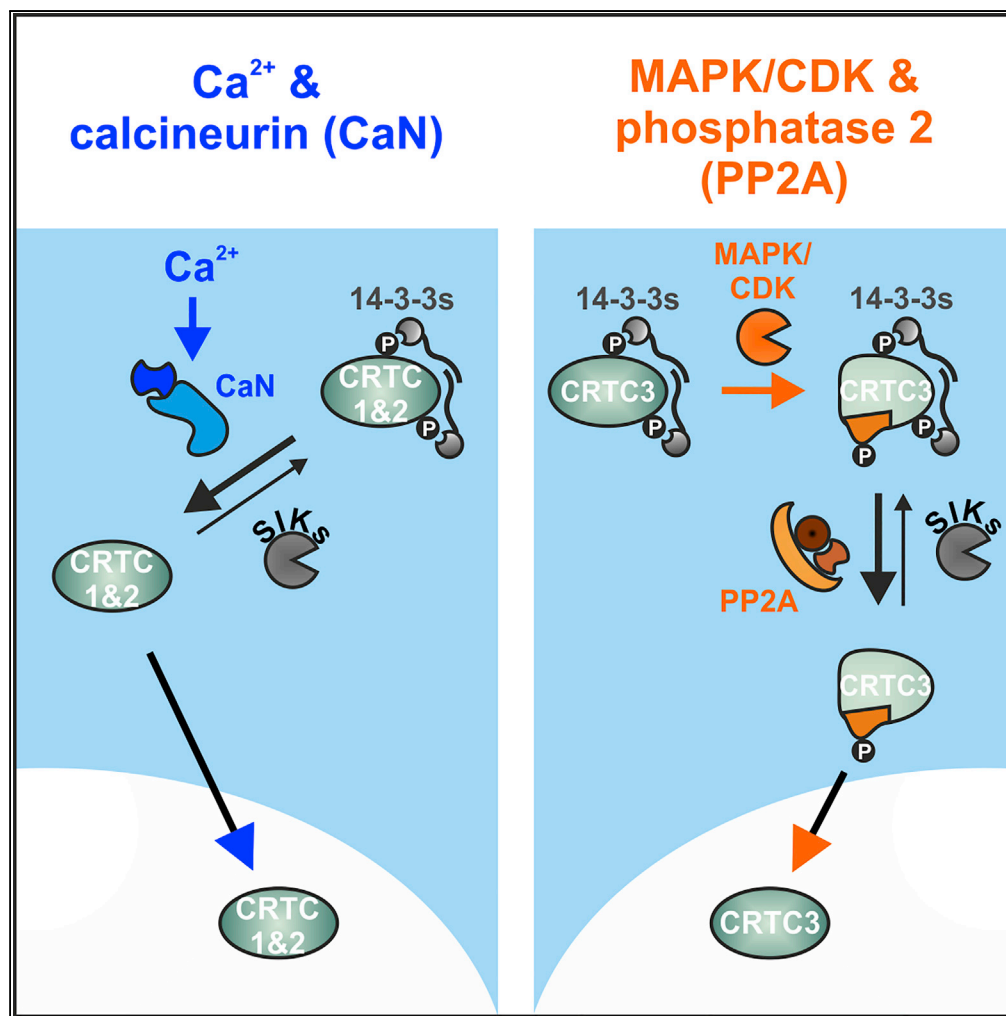


## Article

## Mitogenic Signals Stimulate the CREB Coactivator CRTC3 through PP2A Recruitment



Tim Sonntag,  
Jelena Ostojić,  
Joan M. Vaughan,  
James J. Moresco,  
Young-Sil Yoon,  
John R. Yates III,  
Marc Montminy

montminy@salk.edu

## HIGHLIGHTS

The mammalian CRTC family is distinctly regulated by protein phosphatases

CRTC1 and CRTC2 bind to calcineurin, and PP2A is recruited to CRTC3

CRTC3-PP2A complex formation is mediated by phosphorylation at S391 of CRTC3

Mitogenic signals induce S391 phosphorylation via MAPKs and CDKs

Sonntag et al., iScience 11,  
134–145  
January 25, 2019 © 2019 The  
Authors.  
[https://doi.org/10.1016/  
j.isci.2018.12.012](https://doi.org/10.1016/j.isci.2018.12.012)

## Article

# Mitogenic Signals Stimulate the CREB Coactivator CRTC3 through PP2A Recruitment

Tim Sonntag,<sup>1</sup> Jelena Ostojić,<sup>1</sup> Joan M. Vaughan,<sup>1</sup> James J. Moresco,<sup>2</sup> Young-Sil Yoon,<sup>1</sup> John R. Yates III,<sup>2</sup> and Marc Montminy<sup>1,3,\*</sup>

## SUMMARY

The second messenger 3',5'-cyclic adenosine monophosphate (cAMP) stimulates gene expression via the cAMP-regulated transcriptional coactivator (CRTC) family of cAMP response element-binding protein coactivators. In the basal state, CRTCs are phosphorylated by salt-inducible kinases (SIKs) and sequestered in the cytoplasm by 14-3-3 proteins. cAMP signaling inhibits the SIKs, leading to CRTC dephosphorylation and nuclear translocation. Here we show that although all CRTCs are regulated by SIKs, their interactions with Ser/Thr-specific protein phosphatases are distinct. CRTC1 and CRTC2 associate selectively with the calcium-dependent phosphatase calcineurin, whereas CRTC3 interacts with B55 PP2A holoenzymes via a conserved PP2A-binding region (amino acids 380–401). CRTC3-PP2A complex formation was induced by phosphorylation of CRTC3 at S391, facilitating the subsequent activation of CRTC3 by dephosphorylation at 14-3-3 binding sites. As stimulation of mitogenic pathways promoted S391 phosphorylation via the activation of ERKs and CDKs, our results demonstrate how a ubiquitous phosphatase enables cross talk between growth factor and cAMP signaling pathways at the level of a transcriptional coactivator.

## INTRODUCTION

The second messenger 3',5'-cyclic adenosine monophosphate (cAMP) is a potent driver of cellular responses to hormonal and environmental cues (Montminy, 1997). cAMP mediates the activation of the protein kinase A (PKA) holoenzyme (Taylor et al., 2012), which subsequently phosphorylates cellular substrates (Shabb, 2001). The transcriptional response to cAMP proceeds via the PKA-mediated phosphorylation of cAMP response element (CRE)-binding protein (CREB) family members (CREB1, ATF1, and CREM) (Mayr and Montminy, 2001). Phosphorylation of CREB at S133 induces a conformational change that enables the association of CREB with the histone acetyltransferases CREB-binding protein (CBP) and p300 (Parker et al., 1996). In parallel, cAMP also stimulates the association of CREB with the family of cAMP-regulated transcriptional coactivators (CRTCs, CRTC1–3) over relevant genomic CREB-binding sites (CRE sites) (Altarejos and Montminy, 2011).

Under basal conditions 5' AMP-activated protein kinase family members, most notably the salt-inducible kinases (SIKs, SIK1–3), sequester the three CRTCs in the cytoplasm by phosphorylation at conserved sites, which promotes phosphorylation-dependent 14-3-3 protein binding (Sonntag et al., 2017; Wein et al., 2018). cAMP stimulation triggers the PKA-mediated phosphorylation and inhibition of SIK1–3 (Sonntag et al., 2018), leading to the dephosphorylation of CRTCs, which shuttle to the nucleus and drive cAMP/CREB target gene expression (Wein et al., 2018).

In addition to their regulation by SIKs, CRTCs are also controlled by calcium signaling via the Ca<sup>2+</sup>/calmodulin-dependent protein phosphatase calcineurin (CaN) (Perrino et al., 1995), which binds to and dephosphorylates the CRTCs at 14-3-3 binding sites (Altarejos and Montminy, 2011). The most abundant cellular phosphatases protein phosphatase 1 (PP1) and PP2A also appear to stimulate the dephosphorylation of CRTC2 (Shi, 2009; Uebi et al., 2010), although the context in which these ubiquitous enzymes regulate CRTC activities is unclear.

Multiple CRTC family members are co-expressed in mammalian tissues: CRTC1 and CRTC2 are produced in the brain (Altarejos et al., 2008; Jeanneteau et al., 2012) and pancreatic islets (Eberhard et al., 2013; Malm

<sup>1</sup>Clayton Foundation Laboratories for Peptide Biology, The Salk Institute for Biological Studies, La Jolla, CA 92037, USA

<sup>2</sup>Department of Molecular Medicine, The Scripps Research Institute, La Jolla, CA 92037, USA

<sup>3</sup>Lead Contact

\*Correspondence: montminy@salk.edu

<https://doi.org/10.1016/j.isci.2018.12.012>



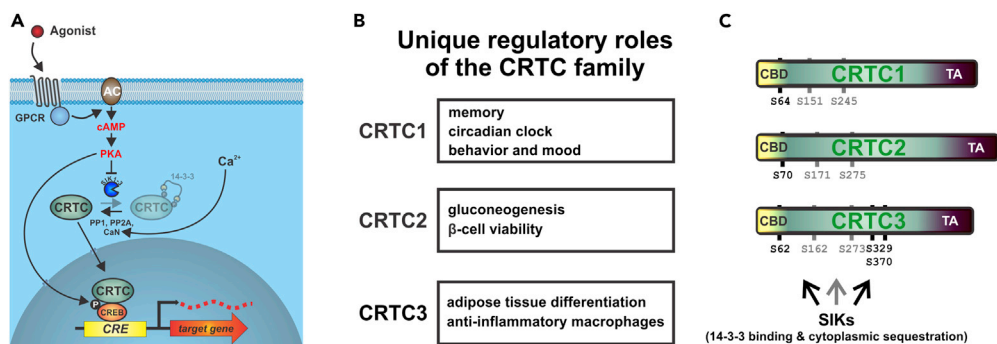


**Figure 1. Common Regulation and Unique Functions of the CRTC Family**

(A) Upon activation of G protein-coupled receptors (GPCRs), cells generate the second messenger cAMP via adenylyl cyclases (ACs). cAMP induces PKA activity, which upon phosphorylation activates CREB and inactivates the SIKs.

Correspondingly, CRTCs are dephosphorylated by the phosphatases PP1 and PP2A and the calcium-responsive CaN, leading to the loss of 14-3-3 protein binding and nuclear translocation. Inside the nucleus, CRTCs bind to CREB over relevant genomic cAMP response element (CRE)-binding sites and drive transcription.

(B) Table lists unique roles of individual CRTC family members.

(C) To-scale representation of the cAMP-regulated transcriptional coactivator (CRTC) protein family (according to *Mus musculus* CRTC proteins). All CRTCs contain multiple salt-inducible kinase (SIK) phosphorylation sites that mediate cytoplasmic sequestration upon 14-3-3 protein binding (black and gray). Two of these sites are conserved and function cooperatively in all CRTCs (gray: S171 and S275 in CRTC2; CBD, CREB-binding domain; TA, transactivation domain).

et al., 2016), for example, whereas CRTC2 and CRTC3 are found in fat (Henriksson et al., 2015; Song et al., 2010), liver (Koo et al., 2005; Patel et al., 2014), and bone marrow-derived immune cells (Kim et al., 2017; MacKenzie et al., 2013). Nevertheless, individual CRTCs appear to execute dominant roles in certain tissues, with CRTC1 controlling memory (Nonaka et al., 2014) and behavior (Breuillaud et al., 2012), entraining the circadian clock (Jagannath et al., 2013), and promoting energy expenditure (Altarejos et al., 2008). By contrast, CRTC2 regulates liver gluconeogenesis (Koo et al., 2005) and beta-cell viability (Blanchet et al., 2015; Eberhard et al., 2013), whereas CRTC3 promotes adipose tissue (Song et al., 2010) and anti-inflammatory macrophage function (MacKenzie et al., 2013). However, it is unknown whether these differences reflect the relative abundance or distinct activation properties of CRTC family members in relevant tissues.

Based on the importance of CRTC dephosphorylation for transcriptional activation, we systematically examined the relative association of individual CRTC family members across the mammalian complement of Ser/Thr-specific protein phosphatases by mass spectrometry. We identified selective interactions of CRTC1/2 with CaN and uncovered an unexpected role for PP2A in binding to and activating CRTC3 in response to extracellular signals. These results point to a novel role for PP2A in mediating effects of growth factor cues on the selective activation of a distinct CRTC family member.

## RESULTS

### Selective Binding of Ser/Thr-Specific Protein Phosphatases to CRTC Family Members

Although they are all regulated by cAMP and the SIKs, individual CRTC family members can perform unique roles (Figures 1A and 1B). We hypothesized that these distinct phenotypes reflect in part differences in protein-protein interactions, rather than differences in CRTC protein abundance. In previous immunoprecipitation (IP)-mass spectrometry (MS) studies, we identified two conserved SIK/14-3-3-binding sites that inhibit CRTC activity (Sonntag et al., 2017) (S171 and S275 in CRTC2; Figure 1C). Using the corresponding HEK 293T cell dataset to identify Ser/Thr phosphatases that interact with overexpressed CRTC1–3 (Figures 2A and 2B), we detected the regulatory and catalytic subunits of CaN in IPs of CRTC1 and CRTC2, but not CRTC3 (Figures 2C and 2D). Conversely, CRTC3 but not CRTC1/2 associated very strongly with PP2A holoenzymes; spectral counts for catalytic (PPP2CA/B), scaffold (PPP2R1A/B), and 55-kDa regulatory B (B55, PPP2R2A–D) subunits were more than 10-fold enriched in IPs of CRTC3 relative to CRTC1/2. Other phosphatases (PP1, PP4, and PP6) appeared to associate comparably, albeit weakly with all CRTC family members (Figure S1).

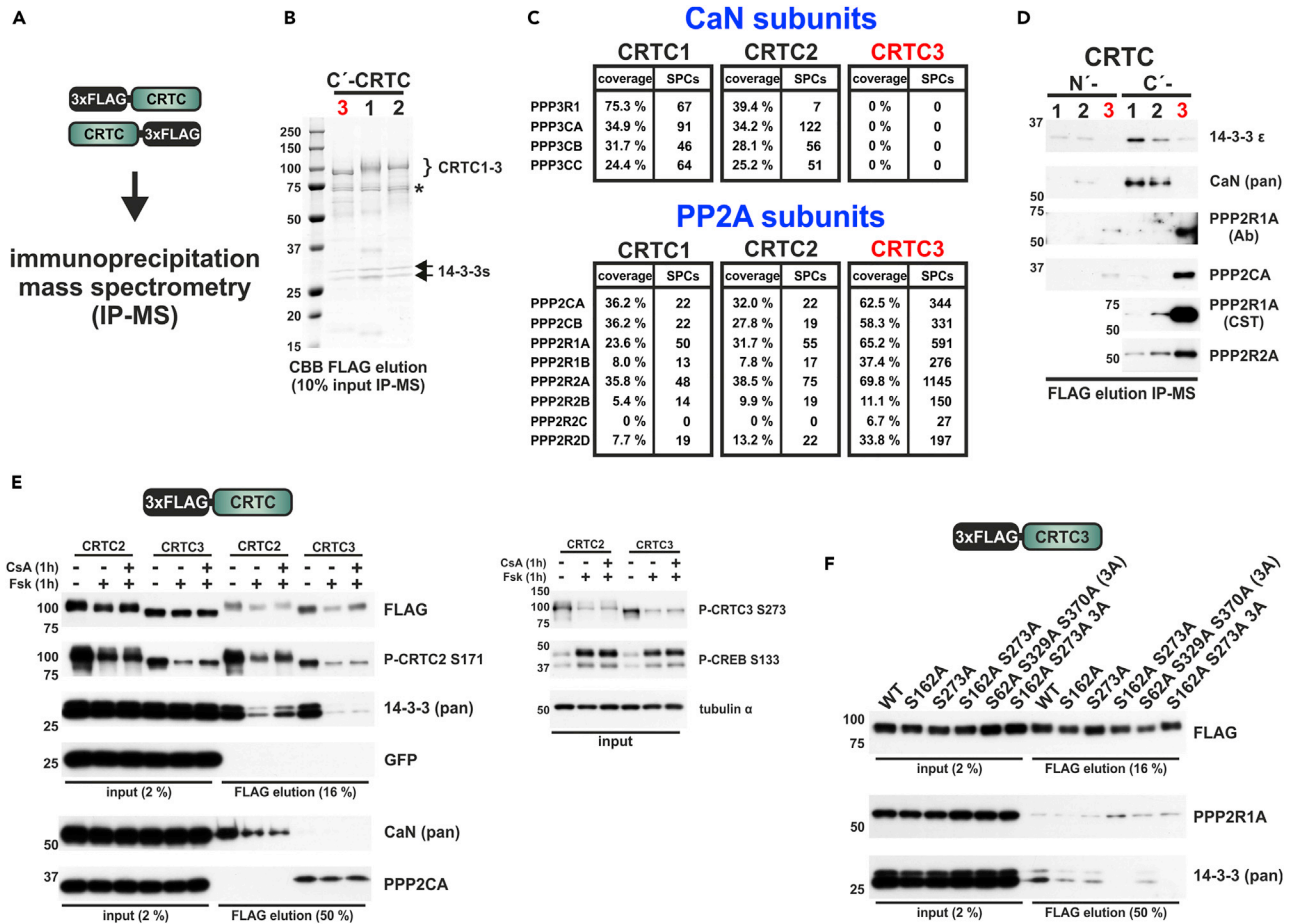


**Figure 2. CRTC Family Members Are Regulated by Distinct Ser/Thr Protein Phosphatases**

(A) Overexpressed N- and C-terminally FLAG-tagged CRTC1–3 were subjected to the immunoprecipitation and mass spectrometry (IP-MS) protocol following exposure to 10  $\mu$ M forskolin (Fsk) for 1 hr.

(B) Coomassie brilliant blue (CBB)-stained SDS-PAGE of colP from C-terminally FLAG-tagged CRTC1–3 subjected to MS (\*, heat shock proteins).

(C) Tables showing recovery of individual subunits from the Ser/Thr phosphatases calcineurin (CaN) and protein phosphatase 2 (PP2A); comparison N-terminally tagged CRTC1–3; SPCs, spectral counts).

(D) Western blot analysis of the MS colP of N- and C-terminally FLAG-tagged CRTC1–3 with endogenous 14-3-3 proteins, CaN, and PP2A (Ab, Abcam; CST, Cell Signaling Technology).

(E) Western blot analysis of the colP of FLAG-tagged CRTC2 and CRTC3 with endogenous 14-3-3 proteins, CaN, and PP2A. One hour before colP, cells were treated with 10  $\mu$ M Fsk and 100 nM cyclosporin (CsA). CRTC2 and CRTC3 were expressed from a plasmid containing the constitutive ubiquitin C promoter (UbC), which drives the expression of EGFP via an internal ribosome entry site. In HEK 293T cells the P-CREB S133 antibody recognizes two bands; the upper band corresponds to CREB1 and the lower band to ATF1 (calculated molecular weight:  $\sim$  37 and 29 kDa).

(F) Western blot analysis of the colP of FLAG-tagged CRTC3 14-3-3 binding site mutants with endogenous 14-3-3s and PP2A.

We confirmed the mutually exclusive interactions of CRTC2 with CaN and CRTC3 with PP2A by co-immunoprecipitation (colP) (Figure 2F). Exposure to the adenylyl cyclase activator forskolin (Fsk) triggered the dephosphorylation of both CRTC2 and CRTC3 at SIK/14-3-3 sites (CRTC2/3: S171/S162 and S275/S273), thereby decreasing their association with 14-3-3 proteins. Co-treatment with the CaN inhibitor cyclosporin (CsA) (Jin and Harrison, 2002) selectively impaired the Fsk-mediated dephosphorylation of CRTC2 at S171, leading to increases in 14-3-3 binding. Fsk stimulation decreased the association of CRTC2 with CaN, but it had no effect on the association of CRTC3 with PP2A. We considered that CRTC3 phosphorylation at 14-3-3 binding sites may modulate PP2A interaction (Figure 2G). Although it eliminated 14-3-3 binding, mutation of all five SIK/14-3-3 sites (Sonntag et al., 2017) in CRTC3 had no effect on its association with PP2A. Collectively, these results indicate that the interaction of CRTC3 with the B55 PP2A holoenzyme is independent of SIK-mediated phosphorylation.

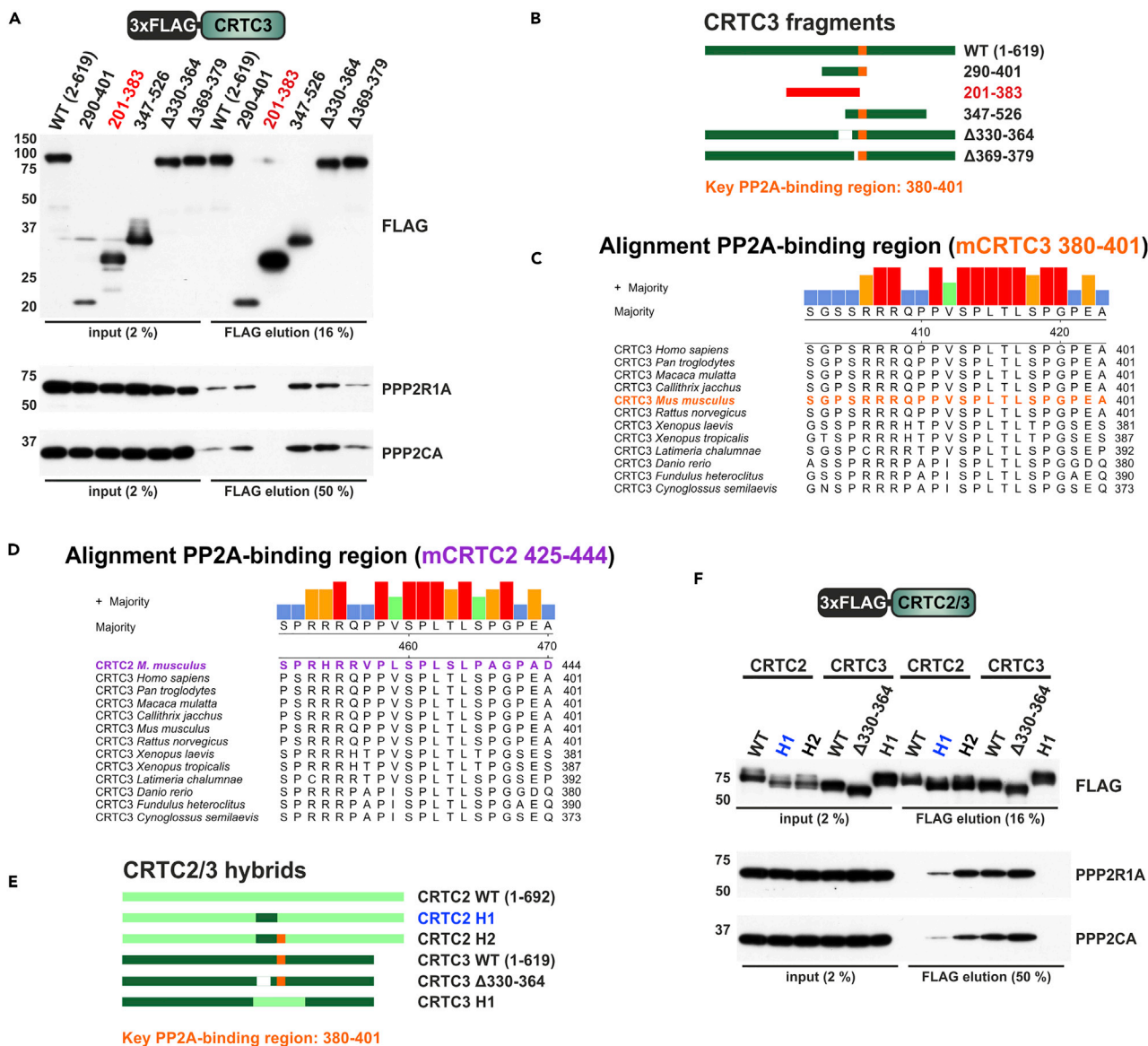


**Figure 3. Characterization of the PP2A-Binding Region (PBR) in CRTC3**

(A) Western blot analysis showing recovery of endogenous PP2A from IPs of FLAG-tagged CRTC3 mutants. The only fragment that abolished PP2A binding is highlighted in red (201–383).  
 (B) To-scale representation of CRTC3 protein fragments assayed for interaction with PP2A. In orange the PBR of CRTC3 (*Mus musculus* amino acids 380–401).  
 (C) CRTC3 sequence alignment of the PBR from multiple vertebrate species (CRTC3 sequences were obtained via UniProt; [The UniProt Consortium, 2017](#)).  
 (D) Sequence alignment of the PBR from vertebrate CRTC3 proteins compared with *M. musculus* CRTC2 425–444 (in purple).  
 (E and F) (E) To-scale representation of the CRTC2 (light green) and CRTC3 (dark green) hybrid proteins assayed for PP2A binding. Hybrid proteins: CRTC2 H1 [mCRTC2(328–421) replaced with mCRTC3(326–379), in blue], CRTC2 H2 [mCRTC2(328–449) replaced with mCRTC3(326–402)], and CRTC3 H1 [mCRTC3(322–407) replaced with mCRTC2(324–454)]. (F) Western blot showing recovery of endogenous PP2A from IPs of FLAG-tagged CRTC2/3 mutants.

**Identification of a Conserved PP2A-Binding Region in CRTC3**

To characterize the PP2A-binding region (PBR) in CRTC3, we generated serial N- and C-terminal truncations of CRTC3 and analyzed these for PP2A association by colP (Figure S2). This analysis uncovered a 20-amino acid core PBR (amino acids 380–401) located within the central regulatory domain of CRTC3 (Figures 3A and 3B). Pointing to an important function for this region, the PBR amino acid sequence is identical between humans and mice (Figure 3C).

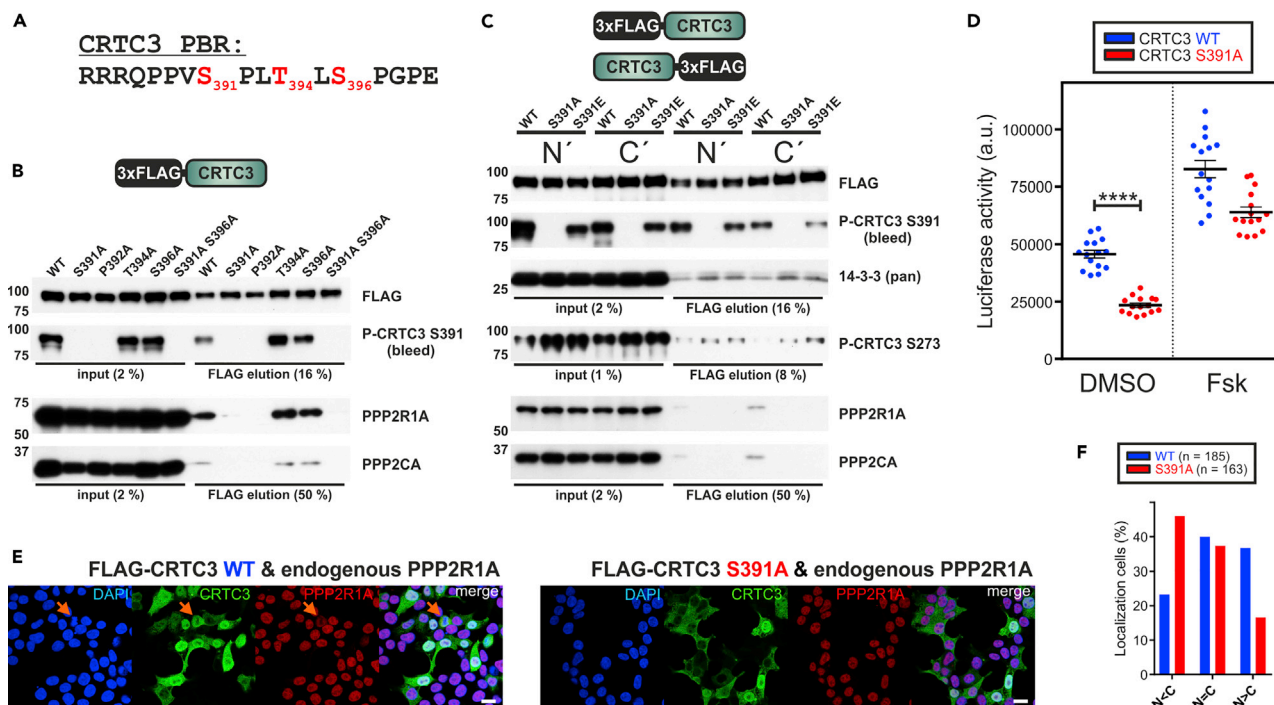


**Figure 4. Phosphorylation of CRT3 at S391 Promotes PP2A Association and CRT3 Activation**

(A) Primary sequence of the PP2A-binding region (PBR) in CRT3 (*H. sapiens* and *Mus musculus* numbering is identical). Phosphorylated residues in red (Hornbeck et al., 2015).

(B) Western blot analysis showing recovery of endogenous PP2A from IPs of FLAG-tagged CRT3 mutants.

(C) Western blot analysis of endogenous PP2A and 14-3-3s recovered from IPs of FLAG-tagged CRT3 S391 mutants.

(D–F) (D) EVX-Luc reporter assay measuring the effect of overexpressed CRT3 wild-type (WT) and S391A mutant upon CREB-dependent gene expression. EVX-Luc activity was measured after 4 hr of DMSO/Fsk treatment (10  $\mu$ M) ( $n = 15$ ,  $\pm$  SEM; \*\*\*\* $p < 0.0001$ ). (E) Immunofluorescence of HEK 293T cells transfected with FLAG-tagged CRT3 WT and S391A. Cells were stained for FLAG epitope, PPP2R1A, and counterstained with DAPI. (Orange arrows depict cells in mitosis; scale bar, 20  $\mu$ m.) (F) Graph depicting the relative subcellular localization of CRT3 WT and S391 mutant (predominantly cytoplasmic [ $N < C$ ], comparable [ $N = C$ ], and predominantly nuclear distribution [ $N > C$ ]).

Although CRT2 does not bind PP2A, it contains a PBR-related sequence at 425–444 (Figure 3D). We generated CRT2/3 hybrids to test whether sequences flanking this core region modulate the PP2A association (Figures 3E and 3F). Similar to the PP2A interaction patterns of truncated CRT3 protein fragments, insertion of mCRT3 326–402 promoted binding of CRT2 to PP2A (CRT2 H2), whereas insertion of the corresponding region of CRT2 (mCRT2 324–454) into CRT3 (CRT3 H1) abolished PP2A binding. However, insertion of CRT3 sequences flanking the PBR into CRT2 (mCRT3 326–379; CRT2 H1) increased PP2A binding to a level that was intermediate between CRT2 and CRT3. These findings indicate that although mCRT3 380–401 is absolutely required for the strong interaction with PP2A, regions outside the PBR also contribute to complex formation.

### Phosphorylation of the PBR Increases PP2A Binding

The CRT3 PBR contains three conserved Ser/Thr residues that appear to undergo phosphorylation (Hornbeck et al., 2015) (Figure 4A). We confirmed the phosphorylation of CRT3 at S391 and S396 by MS analysis (Figure S3). To assess the potential effects of these modifications within the PBR on the CRT3-PP2A interaction, we performed mutagenesis studies (Figure 4B). Although alanine substitutions at T394 and S396 had no effect on PP2A binding, mutation of either S391 or the flanking P392 to alanine abolished this interaction. To monitor phosphorylation at the critical S391 site, we generated a phospho-specific antiserum (P-CRT3 S391). Western blot analysis revealed robust S391 phosphorylation following overexpression of CRT3 wild-type (WT) and T394A or S396A mutant proteins in HEK 293T cells.

To determine the importance of S391 phosphorylation for the CRT3-PP2A interaction, we tested whether substitution of this phosphoacceptor with alanine or a phosphomimetic (Glu) alters complex formation

(Figure 4C). In contrast to WT CRT3, neither S391A nor S391E mutant CRT3 protein associated detectably with PP2A. Correspondingly, phospho-S391-defective CRT3 proteins were phosphorylated to a greater extent at 14-3-3 binding sites (P-CRT3 S273), and as a result, the association of S391A/E mutants with 14-3-3 proteins was stronger compared with WT.

In a transient CRE luciferase-based assay for the quantification of cAMP-dependent gene expression (Conkright et al., 2003), the phosphorylation-defective S391A mutant CRT3 exhibited ~2-fold lower basal transcriptional activity compared with WT CRT3 (Figure 4D). WT and S391A CRT3 CRE activities were more similar following exposure to Fsk, however, suggesting that S391 modulates CRT3 activity in a cAMP-independent manner. We performed immunofluorescence studies to determine the subcellular localization of the S391A mutant (Figures 4E and 4F). In contrast to the predominantly nuclear WT CRT3, S391A mutant protein was primarily localized in the cytoplasm under basal conditions. In keeping with its effects on CRE reporter activity, Fsk promoted the nuclear translocation of CRT3 WT and S391A comparably (Figure S4).

PP2A has multifaceted roles in the cell cycle and is thought to function as a tumor suppressor (Haesen et al., 2014; Wlodarchak and Xing, 2016). Various cellular proteins can inhibit PP2A activity, including the phosphorylation-dependent regulators of mitosis ENSA, ARPP19, and Bod1 (Gharbi-Ayachi et al., 2010; Porter et al., 2013). In contrast to CRT3 (Song et al., 2010), these proteins are small (12–20 kDa) (The UniProt Consortium, 2017) and knockdown or overexpression of any one regulator typically leads to growth arrest and embryonic lethality (Dupre et al., 2014; Matthews and Evans, 2014). Arguing against a role for CRT3 as a PP2A inhibitor, cellular PP2A activity and proliferation appeared comparable between cells expressing WT or phosphorylation-defective (S391A) CRT3 in HEK 293T cells (Figure S5). These results support the notion that S391 phosphorylation selectively increases CRT3 activity by promoting its association with the PP2A holoenzyme, which in turn dephosphorylates CRT3 at remote SIK/14-3-3 sites, leading to CRT3 nuclear translocation and CREB target gene activation.

### MAPKs and CDKs Promote PBR Phosphorylation at S391

Realizing that S391 phosphorylation of CRT3 increases its interaction with PP2A, we set out to identify relevant protein kinases that mediate the phosphorylation of this site. Based on the importance of a flanking proline at the +1 position relative to S391, we addressed the potential involvement of proline-directed kinases in this process by pharmacological inhibition (Figure 5A). Exposure to the cyclin-dependent kinase (CDK1/2/5) inhibitor roscovitine (IC<sub>50</sub>: CDK1/2/5 = 0.2–0.8 μM, ERK1/2 = 15–30 μM) (Meijer et al., 1997) and the ERK1/2 inhibitor SCH772984 (IC<sub>50</sub>: ERK1/2 = 0.004/0.001 μM) (Morris et al., 2013) reduced both CRT3 S391 phosphorylation and PP2A binding following CRT3 overexpression in HEK 293T cells. CDKs (Holt et al., 2009) and mitogen-activated protein kinases (MAPKs) such as ERK1/2 (Carlson et al., 2011) are proline-directed Ser/Thr kinases that appear capable of phosphorylating CRT3 at S391. The CK1α/δ inhibitor longdaysin (IC<sub>50</sub>: CK1α/δ = 6–9 μM, ERK2 = 52 μM) (Hirota et al., 2010) also inhibited S391 phosphorylation, with the PBR (S<sub>391</sub>PLT<sub>394</sub>) containing a casein kinase 1 (CK1) consensus motif pS/Txx(x)S/T (underlined = CK1 phosphorylated residue) (Knippschild et al., 2014). In contrast to its effects on WT CRT3, longdaysin did not impair PP2A binding in the context of the T394A mutant (Figure S6), indicating that S391 and T394 phosphorylation are required for full binding of PP2A in cells overexpressing WT CRT3.

To evaluate the potential role of CDKs in modulating endogenous CRT3 S391 phosphorylation, we arrested HEK 293T cells in the G2/M phase with nocodazole (Figure 5B). Although undetectable in the basal state, phosphorylations of CRT3 at S391 and nucleophosmin (NPM) at T199, a known CDK target (Tokuyama et al., 2001), were both upregulated following nocodazole arrest. Consistent with these effects, short-term CDK inhibition with roscovitine and dinaciclib (IC<sub>50</sub>: CDK1/2/5 = 0.001–0.003 μM) (Parry et al., 2010) blocked the phosphorylation of both proteins.

To test the effect of ERK and cAMP signaling on endogenous S391 phosphorylation of CRT3, we stimulated HEK 293T cells with either 12-O-tetradecanoylphorbol-13-acetate (TPA) (Schonwasser et al., 1998) or Fsk (Figure 5C). In contrast to Fsk, which promoted the dephosphorylation of CRT2 and CRT3 at 14-3-3 sites (P-CRT3 S273: top CRT2 and bottom CRT3), exposure to TPA upregulated ERK activity (P-ERK T202 Y204) and induced CRT3 phosphorylation at S391. These effects were suppressed by pretreatment with the ERK1/2 inhibitor SCH772984.

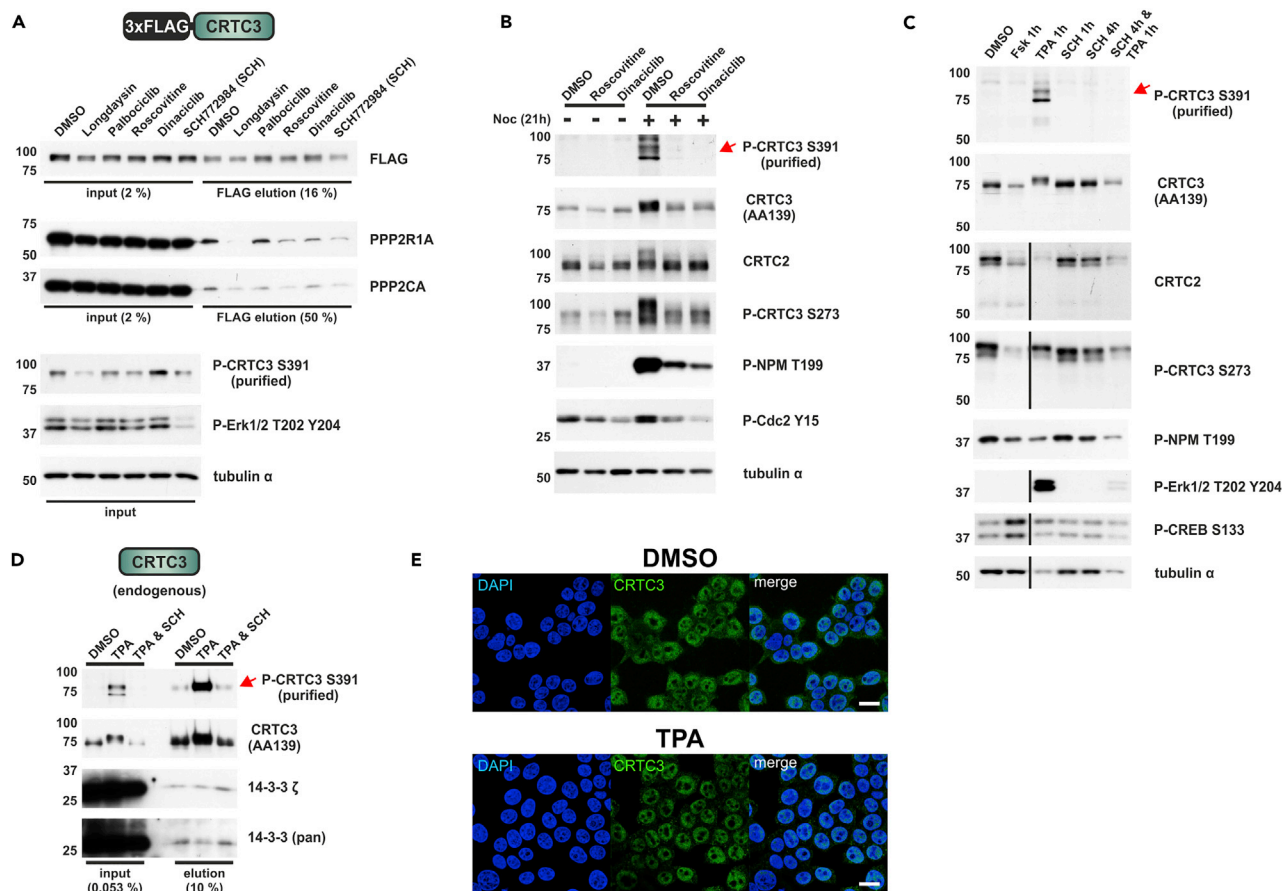


**Figure 5. MAPKs and CDKs Promote S391 Phosphorylation and Activation of CRTC3**

(A) Western blot analysis of endogenous PP2A recovered from IPs of FLAG-tagged CRTC3. Four hours before the IP, HEK 293T cells were treated with small molecule kinase inhibitors: 20  $\mu$ M longdaysin ( $IC_{50}$ :  $CK1\alpha/\delta = 6\text{--}9\ \mu$ M,  $ERK2 = 52\ \mu$ M) (Hirota et al., 2010), 1  $\mu$ M palbociclib ( $IC_{50}$ :  $CDK4/6 = 0.009\text{--}0.015\ \mu$ M) (Fry et al., 2004), 20  $\mu$ M roscovitine ( $IC_{50}$ :  $CDK1/2/5 = 0.2\text{--}0.8\ \mu$ M,  $ERK1/2 = 15\text{--}30\ \mu$ M) (Meijer et al., 1997), 100 nM dinaciclib ( $IC_{50}$ :  $CDK1/2/5 = 0.001\text{--}0.003\ \mu$ M) (Parry et al., 2010), and 100 nM SCH772984 ( $IC_{50}$ :  $ERK1/2 = 0.004/0.001\ \mu$ M) (Morris et al., 2013).

(B) Western blot analysis showing the effects of 21-hr exposure to nocodazole (noc, 0.1  $\mu$ g/mL) on S391 phosphorylation of endogenous CRTC3. Four hours before cell lysis, HEK 293T cells were treated with roscovitine (20  $\mu$ M) and dinaciclib (200 nM). In HEK 293T cells the P-CRTC3 S273 antibody recognizes two bands, the upper band being CRTC2 and the lower band CRTC3 (calculated molecular weight:  $\sim 73$  and 67 kDa).

(C) Western blot analysis showing the effects of 1-hr TPA (200 nM) and Fsk (10  $\mu$ M) treatment on S391 phosphorylation of endogenous CRTC3. In addition, HEK 293T cells were (co-)treated with SCH772984 (SCH; 100 nM) for the indicated time before cell lysis.

(D) Western blot analysis of the coIP of endogenous CRTC3 with 14-3-3 proteins by using the hCRTC3(414-432) antibody. Before the IP, HEK 293T cells were (co-)treated with TPA (200 nM, 1 hr) and SCH772984 (SCH; 200 nM, 2 hr).

(E) Immunofluorescence of HEK 293T cells following 30 minutes of DMSO and TPA (200 nM) stimulation. Cells were stained for endogenous CRTC3 with the hCRTC3(414-432) antibody and counterstained with DAPI (scale bar, 20  $\mu$ m).

Following exposure to TPA or nocodazole, we detected two immunoreactive bands using the S391 phospho-specific antiserum. Both bands correspond to endogenous CRTC3, as revealed in knockdown studies using CRTC3-specific short hairpin RNA (shRNAs) (Figure S7). In previous studies with HEK 293T cells, we found that TPA does not activate the predominant CRTC family member CRTC2 (Ravnskjaer et al., 2007). By contrast, exposure to TPA decreased 14-3-3 protein binding to CRTC3, thereby enhancing its nuclear localization (Figures 5D and 5E). Taken together, these results indicate that MAPKs and CDKs both regulate the S391 phosphorylation and activation of endogenous CRTC3.

### PBR Phosphorylation Increases CRTC3 Activity

Based on the importance of CRTC3 for adipose function (Song et al., 2010; Yoon et al., 2018), we examined CRTC3 S391 phosphorylation in brown-adipose-tissue-derived stromal vascular fraction (bSVF) cells, which are enriched in preadipocytes (Han et al., 2015) (Figure 6A). In the basal state, S391-phosphorylated CRTC3

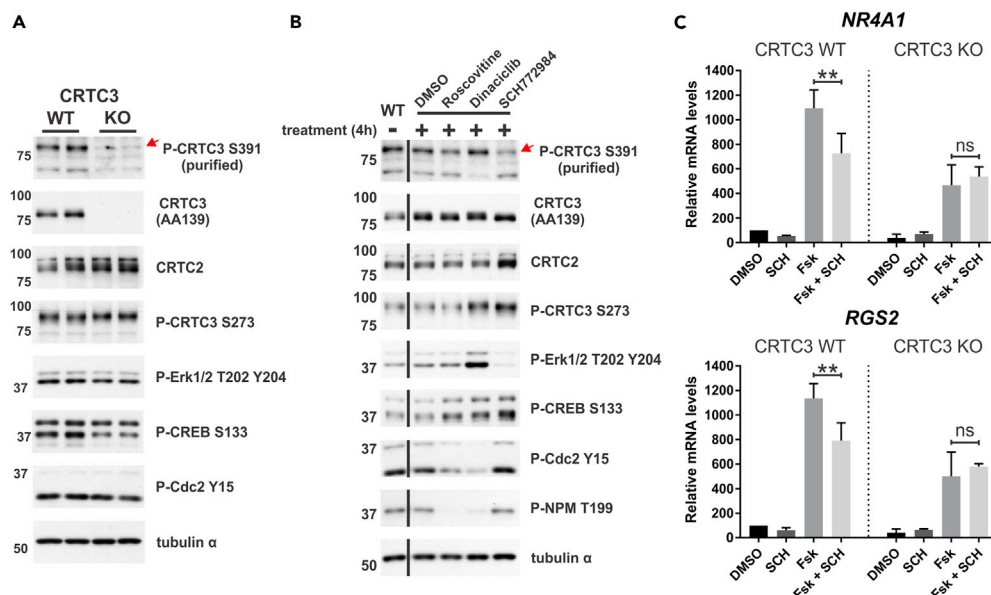


**Figure 6. ERK-Mediated Activation of CRT3 in Undifferentiated bSVFs**

(A) Western blot analysis of primary brown adipose stromal vascular fraction (bSVF) cells generated from wild-type C57BL/6 (WT) and CRTC3 knockout mice (KO).

(B) Western blot analysis showing the effects of 4-hr treatment with roscovitine (20 μM), dinaciclib (200 nM), and SCH772984 (200 nM) on phospho-S391 CRT3 levels in bSVF WT and KO cells.

(C) NR4A1 and RGS2 mRNA levels of bSVF CRT3 WT and KO cells following (co-)treatment with SCH772984 (SCH; 200 nM, 4 hr) and Fsk (10 μM, 1 hr). Values represent data from three independent experiments normalized to RPL32 and relative to CRT3 WT DMSO. (n = 3, ±SD; ns, not statistically significant, \*\*p < 0.01)

was detected in WT, but not in CRTC3 knockout (KO) bSVFs. Having seen their effects on CRTC3 S391 phosphorylation in HEK 293T cells, we tested CDK and ERK inhibitors in bSVFs (Figure 6B). Although both roscovitine and dinaciclib inhibited CDK activity as revealed by the corresponding reduction in NPM T199 phosphorylation, the ERK1/2 inhibitor SCH772984 was most effective in reducing CRTC3 S391 phosphorylation. We evaluated the importance of ERK signaling for CREB target gene expression by exposing bSVFs to SCH772984 (Figure 6C). SCH772984 treatment partially blocked the Fsk-mediated induction of canonical CREB target genes NR4A1 and regulator of G-protein signaling-2 (RGS2) (Ravnskjaer et al., 2007; Song et al., 2010). The inhibitory effects of SCH772984 appear to be CRTC3 dependent, because they were absent in CRTC3 KO bSVFs. Taken together, these results demonstrate that in bSVFs ERK activity functions cooperatively with cAMP/PKA signals to promote CREB target gene expression through its effects on CRTC3.

## DISCUSSION

The second messenger cAMP promotes cellular gene expression via the PKA-mediated phosphorylation and inhibition of the SIKs, leading to CRTC nuclear translocation upon dephosphorylation and release from 14-3-3 proteins (Figure 7A). Here we show that the association of CRTC members with different protein phosphatases provides distinct stimulus-dependent mechanisms for the induction of CREB target genes (Figures 7B and 7C).

The calcium-responsive phosphatase CaN interacts with substrates that contain PxlIT motifs (Li et al., 2011), including vertebrate CRTC1 and CRTC2, but not CRTC3 (mCRTC1: P<sub>219</sub>G<sub>IN</sub>I<sub>F</sub>, P<sub>555</sub>N<sub>I</sub>I<sub>L</sub>T and mCRTC2: P<sub>249</sub>G<sub>IN</sub>I<sub>F</sub>, P<sub>614</sub>N<sub>I</sub>I<sub>L</sub>T). Although PxlIT motifs regulate the substrate affinity of CaN (Li et al., 2007; Roy et al., 2007), its phosphatase activity is dependent upon Ca<sup>2+</sup>/calmodulin (Perrino et al., 1995). As a result, the Ca<sup>2+</sup>/CaN-dependent regulation is limited to CRTC1 and CRTC2 (Altarejos et al., 2008; Kovacs et al., 2007; Screaton et al., 2004; Bittinger et al., 2004; Ch'ng et al., 2012).

By contrast, CRTC3 binds to the B55 PP2A holoenzyme following phosphorylation of CRTC3 at S391 by MAPK/CDKs. Within the PBR (mCRTC3 PBR: 380–401) the S391 phosphorylation site (PVS<sub>391</sub>P) forms part

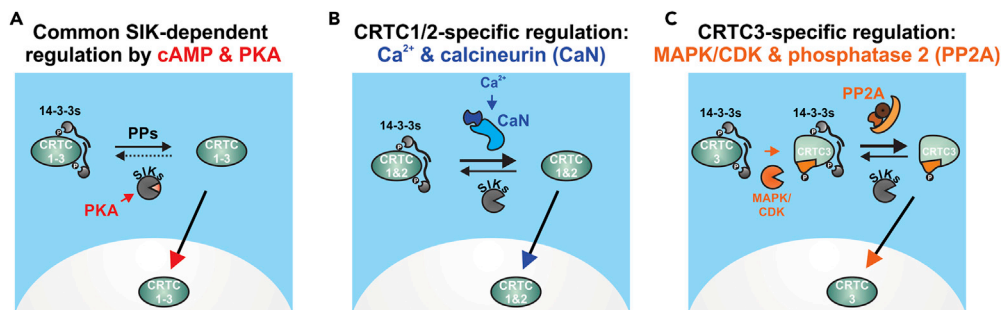


**Figure 7. Differential Regulation of CRTC Family Members by Calcineurin and B55 PP2A**

(A) Scheme depicting the cAMP-dependent regulation of CRTC1–3. In the basal state, SIK-mediated phosphorylation sequesters the CRTCs in the cytoplasm by inducing 14-3-3 interactions. Upon cAMP stimulation, PKA-mediated phosphorylation inactivates the SIKs. CRTCs are dephosphorylated by protein phosphatases (PPs), lose 14-3-3 binding, and translocate to the nucleus.

(B) Scheme depicting the regulation of CRTC1 and CRTC2 by calcineurin. Upon Ca<sup>2+</sup> stimulation, increased calcineurin activity dephosphorylates 14-3-3 binding sites, leading to nuclear translocation of CRTC1/2.

(C) Scheme depicting the regulation of CRTC3 by PP2A. Phosphorylation by MAPKs or CDKs at S391 within the PBR (amino acids 380–401) of CRTC3 enables B55 PP2A holoenzyme recruitment and subsequent dephosphorylation of CRTC3 at 14-3-3 binding sites.

of an optimal ERK1/2 motif (Px[S/T]P) (Carlson et al., 2011). The PBR also contains an MAPK docking motif (D domain), with characteristic basic and alternating hydrophobic residues (RRRQPPV<sub>S391</sub>PLT<sub>L</sub>) (Remenyi et al., 2005). Stimuli that upregulate ERK activity (epidermal growth factor and angiotensin II), also promote the phosphorylation of CRTC3 at S391/S396 (Olsen et al., 2006; Christensen et al., 2010). Superimposed on effects of ERKs, CDKs also appear to phosphorylate CRTC3 at S391 in growth-arrested cells (Olsen et al., 2010; Franz-Wachtel et al., 2012). Indeed, CRTC3 was also identified in a study of mitotic phosphorylation substrates within the chromosomal passenger complex (Yang et al., 2007), which controls cell division together with the CDKs (Carmena et al., 2012). Consistent with the importance of PP2A-mediated activation of CRTC3, in primary calvarial osteoblasts the parathyroid-hormone-induced nuclear translocation of CRTCs was blocked by the PP2A/PP1 inhibitor okadaic acid in case of CRTC3, but not for CRTC2 (Ricarte et al., 2018).

Although the regulatory subunits of PP2A appear important in distinguishing between different substrates, relevant substrate recognition motifs for the PP2A holoenzyme have not been reported until recently (Hansen et al., 2014; Wlodarchak and Xing, 2016). The B55 PP2A holoenzyme has been found to recognize substrates containing a CDK1 phosphorylation site flanked on both sides by a polybasic region (Cundell et al., 2016); a short LxxIxE motif appears to mediate interaction with the B56 PP2A holoenzyme (Hertz et al., 2016). The PBR of CRTC3 includes an N-terminal Arg triplet but lacks any basic C-terminal sequences (mCRTC3: RRRQPPV<sub>S391</sub>PLT<sub>L</sub>SPGPE). Only B55 PP2A subunits were recovered from IPs of all CRTCs, which contain a common sequence inside their PBR-related region consisting of two hydrophobic residues flanking an SP motif (mCRTC1/2/3: PLS<sub>332</sub>PITQ/PLS<sub>434</sub>PLSL/PVS<sub>391</sub>PLTL). Although it lacks an essential glutamate at position 6, this common PBR-like motif in CRTC family members bears more similarity with the LxxIxE motif described for the B56 PP2A holoenzyme. Similar to our findings, phosphorylation of residues within the LxxIxE motif also increases B56 PP2A affinity, leading to the dephosphorylation of distal residues in relevant substrates such as Repo-Man (L<sub>S</sub>PIPE), BubR1 (L<sub>S</sub>PIIE), and RacGAP1 (L<sub>S</sub>TIDE; underlined = phosphorylated residues) (Hertz et al., 2016; Qian et al., 2013; Kruse et al., 2013). Future biochemical studies should reveal the extent to which the PBR we identified represents a distinct binding motif for the B55 PP2A holoenzyme.

The second messenger cAMP is traditionally thought to inhibit cell division, but in a subset of tissues, cAMP appears to cooperate with MAPK/ERK signals in promoting proliferation and differentiation (Dumaz and Marais, 2005). This cross talk is noteworthy in adipose tissue wherein  $\beta$ -adrenergic signaling triggers the activation of both cAMP and MAPK signaling pathways (Collins, 2011), often in combination with growth factors such as insulin/insulin growth factor-1 (Kajimura et al., 2015; Tang and Lane, 2012). As loss of CRTC3 expression increases brown adipocyte proliferation and differentiation and protects against high-fat-diet-induced adipose expansion (Song et al., 2010; Yoon et al., 2018), future studies should

address the specific roles of S391 phosphorylation in this context. This cooperative effect of cAMP and MAPK signals on CRT3 activity has also been reported in regulatory macrophages where lipopolysaccharides (LPS) and prostaglandin E2 (PGE2) promote expression of the anti-inflammatory interleukin 10 (Clark et al., 2012; MacKenzie et al., 2013). Based on the ability of PGE2 to stimulate the cAMP pathway and LPS to activate multiple MAPK family members (Symons et al., 2006), our results suggest that these CRT3-specific effects proceed via the recruitment of B55 PP2A.

### Limitations of the Study

We used HEK 293T cells to characterize CRT3-PP2A complex formation and its regulation by MAPK- and CDK-mediated phosphorylation. Although this approach was valuable in characterizing these molecular components and their downstream effects on CRT3 activation, the relevant extracellular signals that act upstream to trigger the interaction of CRT3 with PP2A remain relatively unknown. Our studies with brown pre-adipocytes support a potential role for ERK in mediating effects of  $\beta$ -adrenergic signals on recruitment of PP2A and on the subsequent activation of CRT3. Future studies with phospho (S391)-specific antiserum should reveal the physiological contexts in which this site is phosphorylated, and mutant mice expressing phospho-S391 defective CRT3 should provide insight into the physiological importance of this modification.

### METHODS

All methods can be found in the accompanying [Transparent Methods supplemental file](#).

### SUPPLEMENTAL INFORMATION

Supplemental Information includes Transparent Methods and seven figures and can be found with this article online at <https://doi.org/10.1016/j.isci.2018.12.012>.

### ACKNOWLEDGMENTS

This work was supported by NIH grant R01 DK083834, the Leona M. and Harry B. Helmsley Charitable Trust, the Clayton Foundation for Medical Research, the Kieckhefer Foundation, NIH-NCI CCSG: P30 014195, NINDS Neuroscience Core Grant: NS072031, and the Waitt Foundation. J.J.M. and J.R.Y. were supported by the National Institute of General Medical Sciences (8 P41 GM103533).

### AUTHOR CONTRIBUTIONS

T.S. conceived the study, designed and performed experiments, analyzed data, and wrote the manuscript. J.O. performed SVF mRNA experiments, analyzed data, provided reagents (CRT3 shRNA plasmids), and edited the manuscript. J.M.V. generated antisera for P-CRT3 S391 (PBL #7408), hCRT3 (PBL #7019), and mCRT2 (PBL #6,896). J.J.M. and J.R.Y. performed MS experiments and data analysis. Y.-S.Y. provided SVF cells. M.M. conceived the study and reviewed/edited the manuscript. All authors reviewed results and approved the final version of the manuscript.

### DECLARATION OF INTERESTS

The authors declare no competing interests.

Received: July 25, 2018

Revised: October 12, 2018

Accepted: December 13, 2018

Published: January 25, 2019

### REFERENCES

- Altarejos, J.Y., Goebel, N., Conkright, M.D., Inoue, H., Xie, J., Arias, C.M., Sawchenko, P.E., and Montminy, M. (2008). The Creb1 coactivator *Crtc1* is required for energy balance and fertility. *Nat. Med.* *14*, 1112–1117.
- Altarejos, J.Y., and Montminy, M. (2011). CREB and the CRT3 co-activators: sensors for hormonal and metabolic signals. *Nat. Rev. Mol. Cell Biol.* *12*, 141–151.
- Bittinger, M.A., McWhinnie, E., Meltzer, J., Iourgenko, V., Latario, B., Liu, X., Chen, C.H., Song, C., Garza, D., and Labow, M. (2004). Activation of cAMP response element-mediated gene expression by regulated nuclear transport of TORC proteins. *Curr. Biol.* *14*, 2156–2161.
- Blanchet, E., van de Velde, S., Matsumura, S., Hao, E., Lelay, J., Kaestner, K., and Montminy, M. (2015). Feedback inhibition of CREB signaling promotes beta cell dysfunction in insulin resistance. *Cell Rep.* *10*, 1149–1157.
- Breuillaud, L., Rossetti, C., Meylan, E.M., Merinat, C., Halfon, O., Magistretti, P.J., and Cardinaux, J.R. (2012). Deletion of CREB-regulated

- transcription coactivator 1 induces pathological aggression, depression-related behaviors, and neuroplasticity genes dysregulation in mice. *Biol. Psychiatry* 72, 528–536.
- Carlson, S.M., Chouinard, C.R., Labadorf, A., Lam, C.J., Schmelzle, K., Fraenkel, E., and White, F.M. (2011). Large-scale discovery of ERK2 substrates identifies ERK-mediated transcriptional regulation by ETV3. *Sci. Signal.* 4, rs11.
- Carmena, M., Wheelock, M., Funabiki, H., and Earnshaw, W.C. (2012). The chromosomal passenger complex (CPC): from easy rider to the godfather of mitosis. *Nat. Rev. Mol. Cell Biol.* 13, 789–803.
- Ch'ng, T.H., Uzgil, B., Lin, P., Avliyakov, N.K., O'dell, T.J., and Martin, K.C. (2012). Activity-dependent transport of the transcriptional coactivator CRTCC1 from synapse to nucleus. *Cell* 150, 207–221.
- Christensen, G.L., Kelstrup, C.D., Lyngso, C., Sarwar, U., Bogebo, R., Sheikh, S.P., Gammeltoft, S., Olsen, J.V., and Hansen, J.L. (2010). Quantitative phosphoproteomics dissection of seven-transmembrane receptor signaling using full and biased agonists. *Mol. Cell. Proteomics* 9, 1540–1553.
- Clark, K., MacKenzie, K.F., Petkevicius, K., Kristariyanto, Y., Zhang, J., Czhoi, H.G., Peggie, M., Plater, L., Pedrioli, P.G., Mciver, E., et al. (2012). Phosphorylation of CRTCC3 by the salt-inducible kinases controls the interconversion of classically activated and regulatory macrophages. *Proc. Natl. Acad. Sci. U S A* 109, 16986–16991.
- Collins, S. (2011).  $\beta$ -adrenoceptor signaling networks in adipocytes for recruiting stored fat and energy expenditure. *Front. Endocrinol. (Lausanne)* 2, 102.
- Conkright, M.D., Canettieri, G., Srean, R., Guzman, E., Miraglia, L., Hogenesch, J.B., and Montminy, M. (2003). TORCs: transducers of regulated CREB activity. *Mol. Cell* 12, 413–423.
- Cundell, M.J., Hutter, L.H., Nunes Bastos, R., Poser, E., Holder, J., Mohammed, S., Novak, B., and Barr, F.A. (2016). A PP2A-B55 recognition signal controls substrate dephosphorylation kinetics during mitotic exit. *J. Cell Biol.* 214, 539–554.
- Dumaz, N., and Marais, R. (2005). Integrating signals between cAMP and the RAS/RAF/MEK/ERK signalling pathways. Based on the anniversary prize of the Gesellschaft Fur Biochemie und molekularbiologie lecture delivered on 5 July 2003 at the special FEBS meeting in Brussels. *FEBS J.* 272, 3491–3504.
- Dupre, A., Daldello, E.M., Nairn, A.C., Jessup, C., and Haccard, O. (2014). Phosphorylation of ARPP19 by protein kinase A prevents meiosis resumption in *Xenopus* oocytes. *Nat. Commun.* 5, 3318.
- Eberhard, C.E., Fu, A., Reeks, C., and Srean, R.A. (2013). CRTCC2 is required for beta-cell function and proliferation. *Endocrinology* 154, 2308–2317.
- Franz-Wachtel, M., Eisler, S.A., Wahl, S., Carpy, A., Nordheim, A., Pfizenmaier, K., Hausser, A., and Macek, B. (2012). Global detection of protein kinase D-dependent phosphorylation events in nocodazole-treated human cells. *Mol. Cell. Proteomics* 11, 160–170.
- Fry, D.W., Harvey, P.J., Keller, P.R., Elliott, W.L., Meade, M., Trachet, E., Albassam, M., Zheng, X., Leopold, W.R., Pryer, N.K., and Toogood, P.L. (2004). Specific inhibition of cyclin-dependent kinase 4/6 by PD 0332991 and associated antitumor activity in human tumor xenografts. *Mol. Cancer Ther.* 3, 1427–1438.
- Gharbi-Ayachi, A., Labbe, J.C., Burgess, A., Vigneron, S., Strub, J.M., Brioude, E., van-Dorsselaer, A., Castro, A., and Lorca, T. (2010). The substrate of greatwall kinase, Arpp19, controls mitosis by inhibiting protein phosphatase 2A. *Science* 330, 1673–1677.
- Haesen, D., Sents, W., Lemaire, K., Hoorne, Y., and Janssens, V. (2014). The basic biology of PP2A in hematologic cells and malignancies. *Front. Oncol.* 4, 347.
- Han, S., Sun, H.M., Hwang, K.C., and Kim, S.W. (2015). Adipose-derived stromal vascular fraction cells: update on clinical utility and efficacy. *Crit. Rev. Eukaryot. Gene Expr.* 25, 145–152.
- Henriksson, E., Sall, J., Gormand, A., Wasserstrom, S., Morrice, N.A., Fritzen, A.M., Foretz, M., Campbell, D.G., Sakamoto, K., Ekelund, M., et al. (2015). SIK2 regulates CRTCCs, HDAC4 and glucose uptake in adipocytes. *J. Cell Sci.* 128, 472–486.
- Hertz, E.P.T., Kruse, T., Davey, N.E., Lopez-Mendez, B., Sigurethsson, J.O., Montoya, G., Olsen, J.V., and Nilsson, J. (2016). A conserved motif provides binding specificity to the PP2A-B56 phosphatase. *Mol. Cell* 63, 686–695.
- Hirota, T., Lee, J.W., Lewis, W.G., Zhang, E.E., Breton, G., Liu, X., Garcia, M., Peters, E.C., Etchegaray, J.P., Traver, D., et al. (2010). High-throughput chemical screen identifies a novel potent modulator of cellular circadian rhythms and reveals CK1 $\alpha$  as a clock regulatory kinase. *PLoS Biol.* 8, e1000559.
- Holt, L.J., Tuch, B.B., Villen, J., Johnson, A.D., Gygi, S.P., and Morgan, D.O. (2009). Global analysis of Cdk1 substrate phosphorylation sites provides insights into evolution. *Science* 325, 1682–1686.
- Hornbeck, P.V., Zhang, B., Murray, B., Kornhauser, J.M., Latham, V., and Skrzypek, E. (2015). PhosphoSitePlus, 2014: mutations, PTMs and recalibrations. *Nucleic Acids Res.* 43, D512–D520.
- Jagannath, A., Butler, R., Godinho, S.I., Couch, Y., Brown, L.A., Vasudevan, S.R., Flanagan, K.C., Anthony, D., Churchill, G.C., Wood, M.J., et al. (2013). The CRTCC1-SIK1 pathway regulates entrainment of the circadian clock. *Cell* 154, 1100–1111.
- Jeanneteau, F.D., Lambert, W.M., Ismaili, N., Bath, K.G., Lee, F.S., Garabedian, M.J., and Chao, M.V. (2012). BDNF and glucocorticoids regulate corticotrophin-releasing hormone (CRH) homeostasis in the hypothalamus. *Proc. Natl. Acad. Sci. U S A* 109, 1305–1310.
- Jin, L., and Harrison, S.C. (2002). Crystal structure of human calcineurin complexed with cyclosporin A and human cyclophilin. *Proc. Natl. Acad. Sci. U S A* 99, 13522–13526.
- Kajimura, S., Spiegelman, B.M., and Seale, P. (2015). Brown and beige fat: physiological roles beyond heat generation. *Cell Metab.* 22, 546–559.
- Kim, J.H., Hedrick, S., Tsai, W.W., Wiater, E., Le Lay, J., Kaestner, K.H., Leblanc, M., Loar, A., and Montminy, M. (2017). CREB coactivators CRTCC2 and CRTCC3 modulate bone marrow hematopoiesis. *Proc. Natl. Acad. Sci. U S A* 114, 11739–11744.
- Knippschild, U., Kruger, M., Richter, J., Xu, P., Garcia-Reyes, B., Peifer, C., Halekotte, J., Bakulev, V., and Bischof, J. (2014). The CK1 family: contribution to cellular stress response and its role in carcinogenesis. *Front. Oncol.* 4, 96.
- Koo, S.H., Flechner, L., Qi, L., Zhang, X., Srean, R.A., Jeffries, S., Hedrick, S., Xu, W., Boussouar, F., Brindle, P., et al. (2005). The CREB coactivator TORC2 is a key regulator of fasting glucose metabolism. *Nature* 437, 1109–1111.
- Kovacs, K.A., Steullet, P., Steinmann, M., Do, K.O., Magistretti, P.J., Halfon, O., and Cardinaux, J.R. (2007). TORC1 is a calcium- and cAMP-sensitive coincidence detector involved in hippocampal long-term synaptic plasticity. *Proc. Natl. Acad. Sci. U S A* 104, 4700–4705.
- Kruse, T., Zhang, G., Larsen, M.S., Lischetti, T., Streicher, W., Kragh Nielsen, T., Bjorn, S.P., and Nilsson, J. (2013). Direct binding between BubR1 and B56-PP2A phosphatase complexes regulate mitotic progression. *J. Cell Sci.* 126, 1086–1092.
- Li, H., Rao, A., and Hogan, P.G. (2011). Interaction of calcineurin with substrates and targeting proteins. *Trends Cell Biol.* 21, 91–103.
- Li, H., Zhang, L., Rao, A., Harrison, S.C., and Hogan, P.G. (2007). Structure of calcineurin in complex with PVIVIT peptide: portrait of a low-affinity signalling interaction. *J. Mol. Biol.* 369, 1296–1306.
- MacKenzie, K.F., Clark, K., Naqvi, S., McGuire, V.A., Noehren, G., Kristariyanto, Y., van den Bosch, M., Mudaliar, M., McCarthy, P.C., Pattison, M.J., et al. (2013). PGE(2) induces macrophage IL-10 production and a regulatory-like phenotype via a protein kinase A-SIK-CRTCC3 pathway. *J. Immunol.* 190, 565–577.
- Malm, H.A., Mollet, I.G., Berggreen, C., Orholm-Melander, M., Esguerra, J.L., Goransson, O., and Eliasson, L. (2016). Transcriptional regulation of the miR-212/miR-132 cluster in insulin-secreting beta-cells by cAMP-regulated transcriptional co-activator 1 and salt-inducible kinases. *Mol. Cell. Endocrinol.* 424, 23–33.
- Matthews, L.M., and Evans, J.P. (2014). alpha-endosulfine (ENSA) regulates exit from prophase I arrest in mouse oocytes. *Cell Cycle* 13, 1639–1649.
- Mayr, B., and Montminy, M. (2001). Transcriptional regulation by the phosphorylation-dependent factor CREB. *Nat. Rev. Mol. Cell Biol.* 2, 599–609.
- Meijer, L., Borgne, A., Mulner, O., Chong, J.P., Blow, J.J., Inagaki, N., Inagaki, M., Delcros, J.G., and Moulinoux, J.P. (1997). Biochemical and

- cellular effects of roscovitine, a potent and selective inhibitor of the cyclin-dependent kinases *cdc2*, *cdk2* and *cdk5*. *Eur. J. Biochem.* 243, 527–536.
- Montminy, M. (1997). Transcriptional regulation by cyclic AMP. *Annu. Rev. Biochem.* 66, 807–822.
- Morris, E.J., Jha, S., Restaino, C.R., Dayananth, P., Zhu, H., Cooper, A., Carr, D., Deng, Y., Jin, W., Black, S., et al. (2013). Discovery of a novel ERK inhibitor with activity in models of acquired resistance to BRAF and MEK inhibitors. *Cancer Discov.* 3, 742–750.
- Nonaka, M., Kim, R., Fukushima, H., Sasaki, K., Suzuki, K., Okamura, M., Ishii, Y., Kawashima, T., Kamijo, S., Takemoto-Kimura, S., et al. (2014). Region-specific activation of CRTCC1-CREB signaling mediates long-term fear memory. *Neuron* 84, 92–106.
- Olsen, J.V., Blagoev, B., Gnäd, F., Macek, B., Kumar, C., Mortensen, P., and Mann, M. (2006). Global, in vivo, and site-specific phosphorylation dynamics in signaling networks. *Cell* 127, 635–648.
- Olsen, J.V., Vermeulen, M., Santamaria, A., Kumar, C., Miller, M.L., Jensen, L.J., Gnäd, F., Cox, J., Jensen, T.S., et al. (2010). Quantitative phosphoproteomics reveals widespread full phosphorylation site occupancy during mitosis. *Sci. Signal.* 3, ra3.
- Parker, D., Ferreri, K., Nakajima, T., Lamorte, V.J., Evans, R., Koerber, S.C., Hoeger, C., and Montminy, M.R. (1996). Phosphorylation of CREB at Ser-133 induces complex formation with CREB-binding protein via a direct mechanism. *Mol. Cell. Biol.* 16, 694–703.
- Parry, D., Guzi, T., Shanahan, F., Davis, N., Prabhavalkar, D., Wiswell, D., Seghezzi, W., Paruch, K., Dwyer, M.P., Doll, R., et al. (2010). Dinaciclib (SCH 727965), a novel and potent cyclin-dependent kinase inhibitor. *Mol. Cancer Ther.* 9, 2344–2353.
- Patel, K., Foretz, M., Marion, A., Campbell, D.G., Gourlay, R., Boudaba, N., Tournier, E., Titchenell, P., Pegg, M., Deak, M., et al. (2014). The LKB1-salt-inducible kinase pathway functions as a key gluconeogenic suppressor in the liver. *Nat. Commun.* 5, 4535.
- Perrino, B.A., Ng, L.Y., and Soderling, T.R. (1995). Calcium regulation of calcineurin phosphatase activity by its B subunit and calmodulin. Role of the autoinhibitory domain. *J. Biol. Chem.* 270, 340–346.
- Porter, I.M., Schleicher, K., Porter, M., and Swedlow, J.R. (2013). *Bod1* regulates protein phosphatase 2A at mitotic kinetochores. *Nat. Commun.* 4, 2677.
- Qian, J., Beullens, M., Lesage, B., and Bollen, M. (2013). Aurora B defines its own chromosomal targeting by opposing the recruitment of the phosphatase scaffold Repo-Man. *Curr. Biol.* 23, 1136–1143.
- Ravnskjaer, K., Kester, H., Liu, Y., Zhang, X., Lee, D., Yates, J.R., 3rd, and Montminy, M. (2007). Cooperative interactions between CBP and TORC2 confer selectivity to CREB target gene expression. *EMBO J.* 26, 2880–2889.
- Remenyi, A., Good, M.C., Bhattacharyya, R.P., and Lim, W.A. (2005). The role of docking interactions in mediating signaling input, output, and discrimination in the yeast MAPK network. *Mol. Cell* 20, 951–962.
- Ricarte, F.R., le Henaff, C., Kolupaeva, V.G., Gardella, T.J., and Partridge, N.C. (2018). Parathyroid hormone (1-34) and its analogs differentially modulate osteoblastic RANKL expression via PKA/PP1/PP2A and SIK2/SIK3-CRTC3 signaling. *J. Biol. Chem.*
- Roy, J., Li, H., Hogan, P.G., and Cyert, M.S. (2007). A conserved docking site modulates substrate affinity for calcineurin, signaling output, and in vivo function. *Mol. Cell* 25, 889–901.
- Schonwasser, D.C., Marais, R.M., Marshall, C.J., and Parker, P.J. (1998). Activation of the mitogen-activated protein kinase/extracellular signal-regulated kinase pathway by conventional, novel, and atypical protein kinase C isoforms. *Mol. Cell Biol.* 18, 790–798.
- Screaton, R.A., Conkright, M.D., Katoh, Y., Best, J.L., Canettieri, G., Jeffries, S., Guzman, E., Niessen, S., Yates, J.R., 3rd, Takemori, H., et al. (2004). The CREB coactivator TORC2 functions as a calcium- and cAMP-sensitive coincidence detector. *Cell* 119, 61–74.
- Shabb, J.B. (2001). Physiological substrates of cAMP-dependent protein kinase. *Chem. Rev.* 101, 2381–2411.
- Shi, Y. (2009). Serine/threonine phosphatases: mechanism through structure. *Cell* 139, 468–484.
- Song, Y., Altarejos, J., Goodarzi, M.O., Inoue, H., Guo, X., Berdeaux, R., Kim, J.H., Goode, J., Igata, M., Paz, J.C., et al. (2010). CRTC3 links catecholamine signalling to energy balance. *Nature* 468, 933–939.
- Sonntag, T., Moresco, J.J., Vaughan, J.M., Matsumura, S., Yates, J.R., 3rd, and Montminy, M. (2017). Analysis of a cAMP regulated coactivator family reveals an alternative phosphorylation motif for AMPK family members. *PLoS One* 12, e0173013.
- Sonntag, T., Vaughan, J.M., and Montminy, M. (2018). 14-3-3 proteins mediate inhibitory effects of cAMP on salt-inducible kinases (SIKs). *FEBS J.* 285, 467–480.
- Symons, A., Beinke, S., and Ley, S.C. (2006). MAP kinase kinase kinases and innate immunity. *Trends Immunol.* 27, 40–48.
- Tang, Q.Q., and Lane, M.D. (2012). Adipogenesis: from stem cell to adipocyte. *Annu. Rev. Biochem.* 81, 715–736.
- Taylor, S.S., Ilouz, R., Zhang, P., and Kornev, A.P. (2012). Assembly of allosteric macromolecular switches: lessons from PKA. *Nat. Rev. Mol. Cell Biol.* 13, 646–658.
- The Uniprot Consortium (2017). UniProt: the universal protein knowledgebase. *Nucleic Acids Res.* 45, D158–D169.
- Tokuyama, Y., Horn, H.F., Kawamura, K., Tarapore, P., and Fukasawa, K. (2001). Specific phosphorylation of nucleophosmin on Thr(199) by cyclin-dependent kinase 2-cyclin E and its role in centrosome duplication. *J. Biol. Chem.* 276, 21529–21537.
- Uebi, T., Tamura, M., Horike, N., Hashimoto, Y.K., and Takemori, H. (2010). Phosphorylation of the CREB-specific coactivator TORC2 at Ser(307) regulates its intracellular localization in COS-7 cells and in the mouse liver. *Am. J. Physiol. Endocrinol. Metab.* 299, E413–E425.
- Wein, M.N., Foretz, M., Fisher, D.E., Xavier, R.J., and Kronenberg, H.M. (2018). Salt-inducible kinases: physiology, regulation by cAMP, and therapeutic potential. *Trends Endocrinol. Metab.* 29, 723–735.
- Wlodarchak, N., and Xing, Y. (2016). PP2A as a master regulator of the cell cycle. *Crit. Rev. Biochem. Mol. Biol.* 51, 162–184.
- Yang, F., Camp, D.G., 2nd, Gritsenko, M.A., Luo, Q., Kelly, R.T., Clauss, T.R., Brinkley, W.R., Smith, R.D., and Stenoien, D.L. (2007). Identification of a novel mitotic phosphorylation motif associated with protein localization to the mitotic apparatus. *J. Cell Sci.* 120, 4060–4070.
- Yoon, Y.S., Tsai, W.W., van de Velde, S., Chen, Z., Lee, K.F., Morgan, D.A., Rahmouni, K., Matsumura, S., Wiater, E., Song, Y., and Montminy, M. (2018). cAMP-inducible coactivator CRTC3 attenuates brown adipose tissue thermogenesis. *Proc. Natl. Acad. Sci. U S A* 115, E5289–E5297.

**ISCI, Volume 11**

**Supplemental Information**

**Mitogenic Signals Stimulate  
the CREB Coactivator CRTC3  
through PP2A Recruitment**

**Tim Sonntag, Jelena Ostojić, Joan M. Vaughan, James J. Moresco, Young-Sil Yoon, John R. Yates III, and Marc Montminy**

## Supplemental Figures

Fig. S1

	PP1 subunits						PP4 subunits						PP6 subunits					
	CRTC1		CRTC2		CRTC3		CRTC1		CRTC2		CRTC3		CRTC1		CRTC2		CRTC3	
	coverage	SPCs	coverage	SPCs	coverage	SPCs	coverage	SPCs	coverage	SPCs	coverage	SPCs	coverage	SPCs	coverage	SPCs	coverage	SPCs
PPP1CA	11.8 %	16	9.7 %	16	40.6 %	20	10.7 %	4	20.2 %	7	43.3 %	56	21.3 %	9	11.5 %	3	41.6 %	15
PPP1CB	13.5 %	14	9.8 %	16	37.6 %	18	0 %	0	2.6 %	2	7.0 %	3	0 %	0	0 %	0	3.0 %	2
PPP1CC	8.7 %	7	9.9 %	16	27.9 %	17	6.2 %	5	3.8 %	3	14.4 %	12	4.0 %	8	8.0 %	13	9.8 %	17
PPP1R10	2.3 %	2	5.7 %	3	3.8 %	5												
PPP4C																		
PPP4R2																		
PPP4R3A																		
PPP6C																		
PPP6R1																		
PPP6R3																		

Fig. S1. Interaction of CRTC1-3 with protein phosphatases 1, 4, and 6. Related to Fig. 2.

Tables show the IP-MS recovery of protein phosphatases (PP) 1, 4, and 6 subunits (comparing N-terminally tagged CRTC1-3; SPCs = spectral counts).

Fig. S2

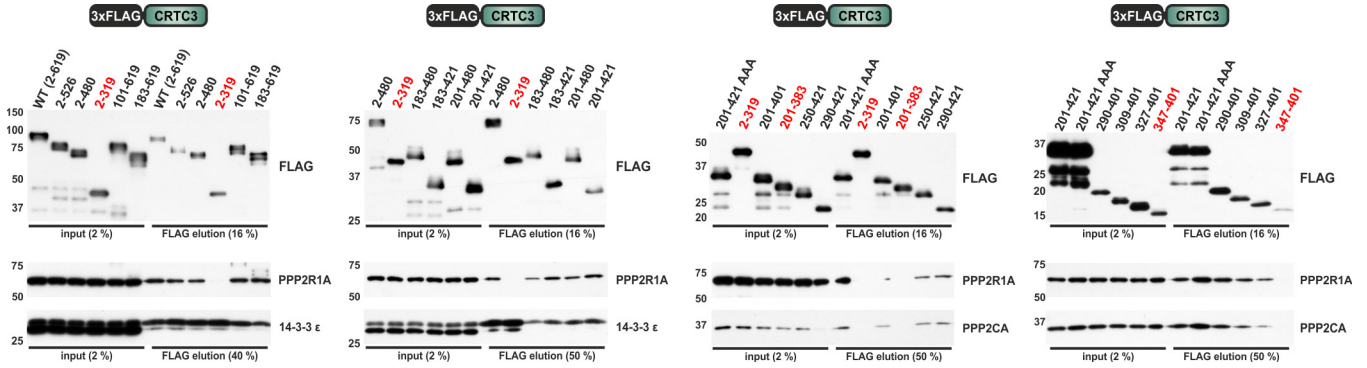
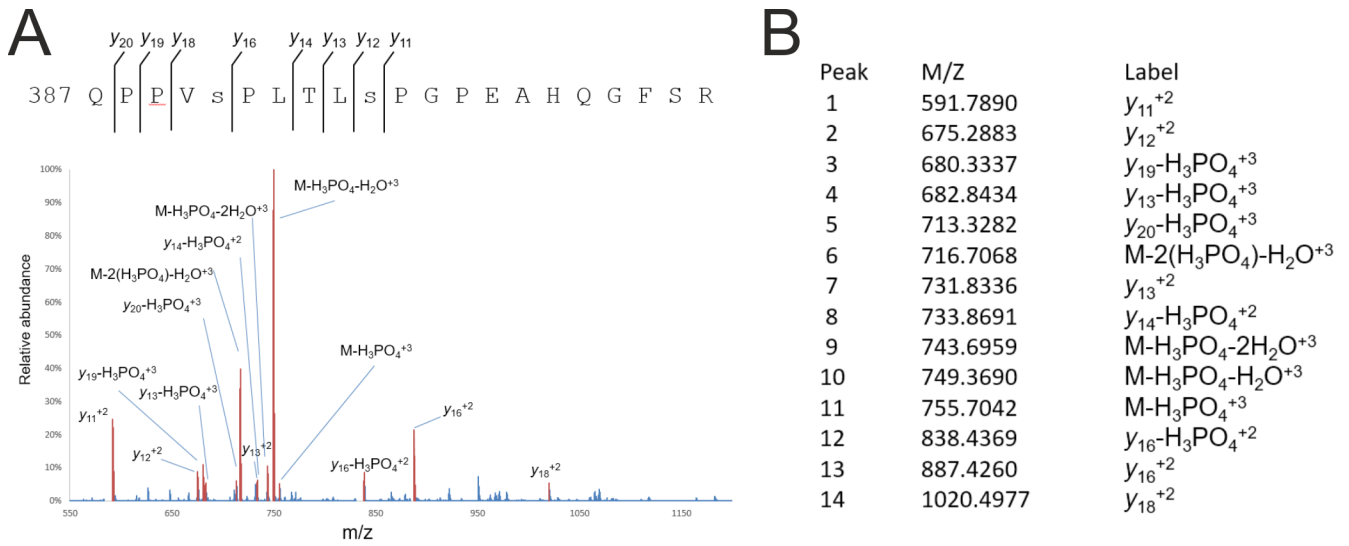


Fig. S2. Characterization of the PP2A-binding region (PBR) in CRTC3. Related to Fig. 3.

Western blot analysis of Co-IPs of FLAG-tagged CRTC3 truncation mutants with endogenous PP2A and 14-3-3 proteins. Mutants that abolished PP2A interaction are highlighted in red (201-421 AAA = mCRTC3 201-421 S273A S329A S370A).

**Fig. S3**



**Fig. S3. Phosphorylation of S391 and S396 within the PP2A-binding region (PBR) of CRTC3.** Related to Fig. 4.

A) Detection of MS spectra (387-407) derived from the PBR with corresponding peaks labeled (in B)). Phosphorylation was detected on amino acid s391 (Ascore = 14.89) and s396 (Ascore = 7.53; for Ascore see (Beausoleil et al., 2006)).

Fig. S4

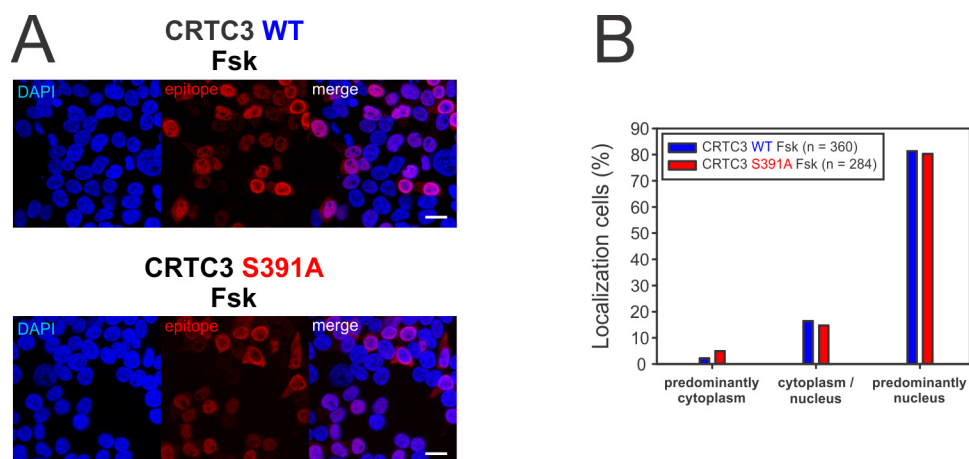


**Fig. S4. Localization of CRTC3 WT and S391A mutant upon Forskolin treatment.** Related to Fig. 4.

A) Immunofluorescence of HEK 293T cells transfected with FLAG-tagged CRTC3 WT and S391A. Cells were stained for FLAG epitope and counterstained with DAPI. (Fsk treatment for 30 min; scale bar indicates 20  $\mu$ m) B) Graph shows relative subcellular localization of CRTC3 WT and S391A mutant.

Fig. S5

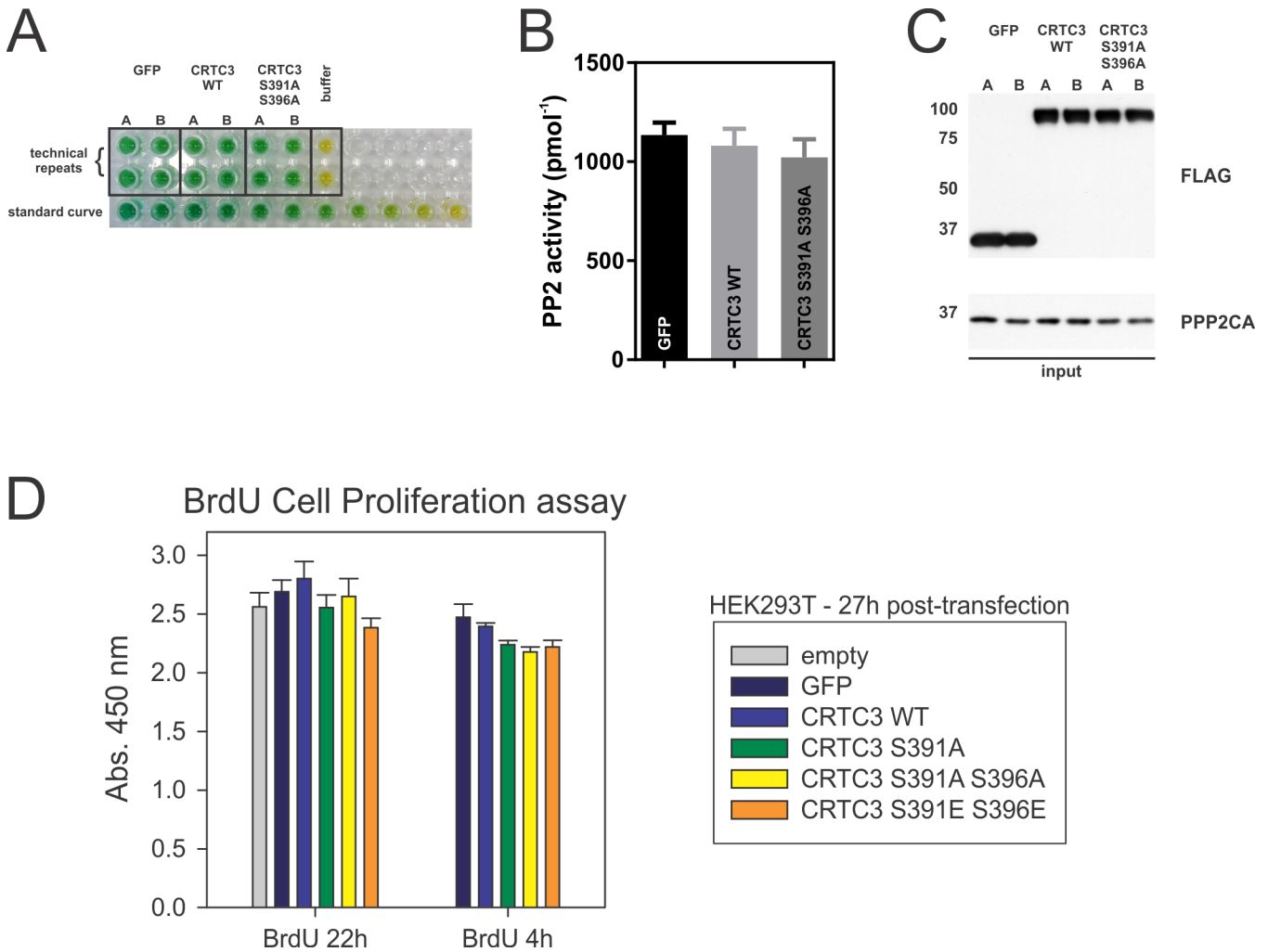


**Fig. S5. Effect of CRTC3 overexpression on cellular PP2A activity and cell proliferation.** Related to Fig. 4.

A-C) The activity of immunoprecipitated catalytic PP2A subunit (PPP2CA) was quantified by malachite green and KRpTIRR phosphopeptide (PP2A Immunoprecipitation Phosphatase Assay Kit, Upstate). Prior to PP2A activity measurement FLAG-tagged GFP, CRTC3 and CRTC3 S391A S396A were overexpressed in HEK 293T cells for 48 h. A) Picture of the 96 well plate after the colorimetric PP2A assay. (A/B indicates independent transfections). B) Corresponding PP2A activity upon normalization to the standard curve. ( $n = 4, \pm$  SD). C) Corresponding Western blot analysis of the cell lysate used for the PP2A activity assay. D) BrdU Cell Proliferation ELISA Kit (Abcam) measuring the effects of transient-overexpression of GFP, CRTC3, and CRTC3

mutants on HEK 293T proliferation. BrdU treatment occurred either for 22 h (5 h post-transfection) or for 4 h (23 h post-transfection) prior to the colorimetric assay. ( $n = 5, \pm \text{SEM}$ ).

Fig. S6

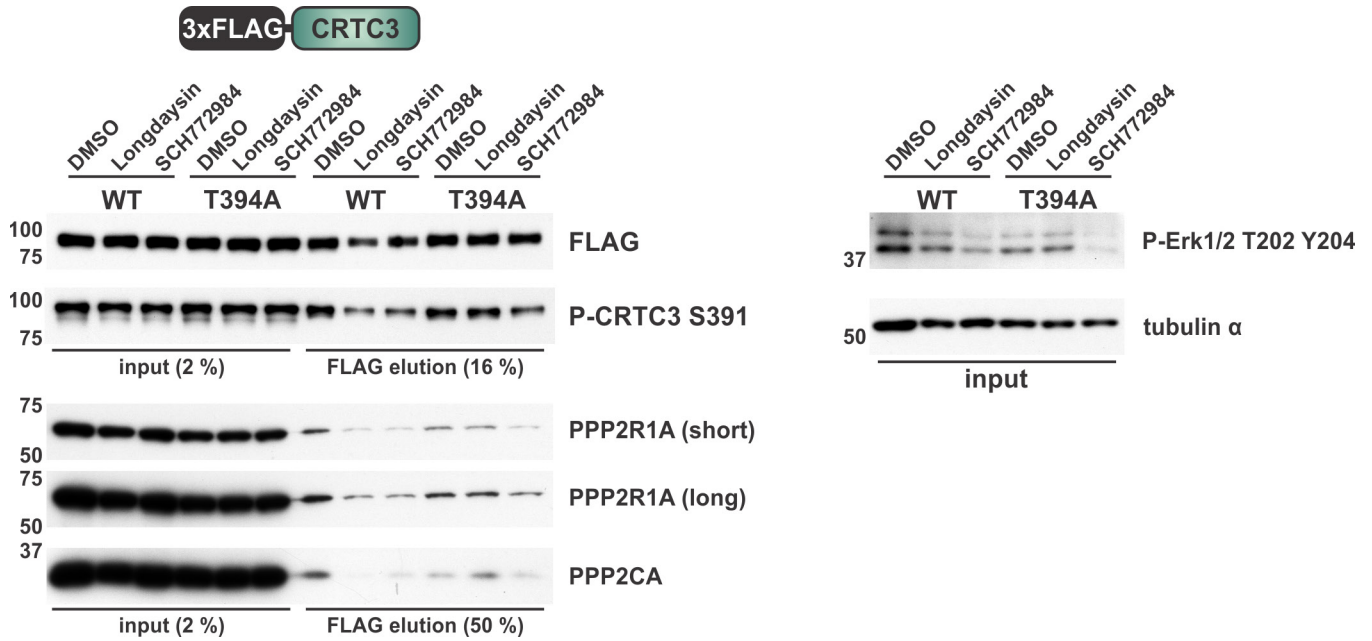


**Fig. S6. The effects of Longdaysin on the CRTC3-PP2A complex formation requires the intact CK1 motif inside the PBR.** Related to Fig. 5.

Western blot analysis of the Co-IP of FLAG-tagged CRTC3 WT and T394A mutant with endogenous PP2A. 4 h prior to the IP HEK 293T cells were treated with Longdaysin (20  $\mu$ M;  $IC_{50}$   $\mu$ M: CK1 $\alpha/\delta$  = 6-9, ERK2 = 52 (Hirota et al., 2010)) and SCH772984 (100 nM;  $IC_{50}$   $\mu$ M: ERK1/2 = 0.004/0.001 (Morris et al., 2013)).

Fig. S7

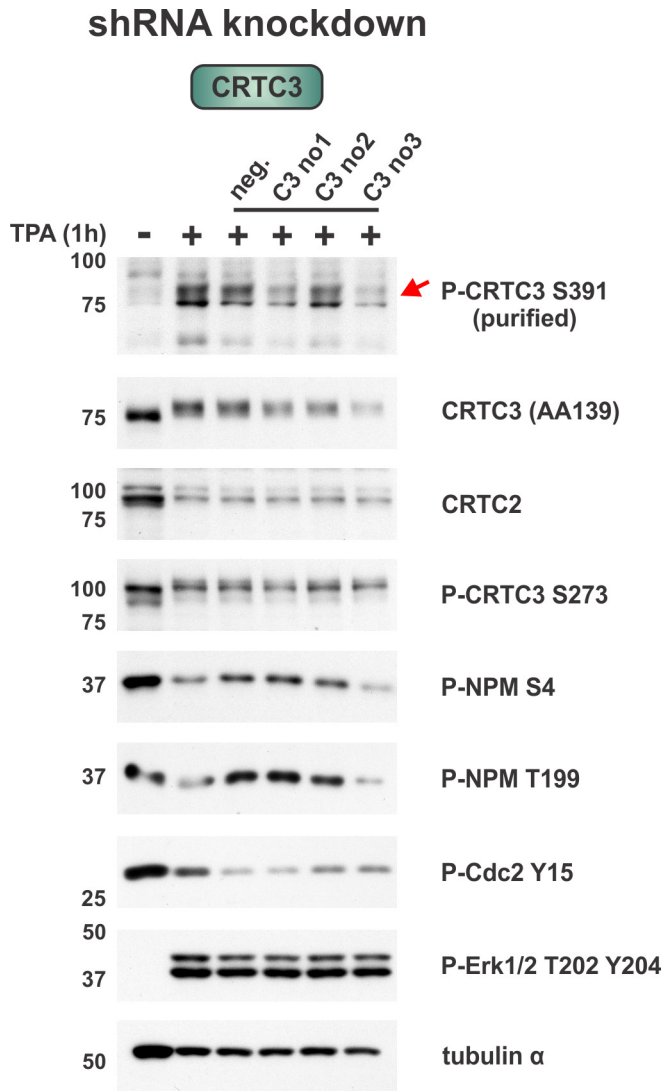


Fig. S7. P-CRTC3 S391 antibody evaluation. Related to Fig. 5.

A) Western blot analysis showing the effects of transient CRTC3 knockdown and TPA treatment (200 nM, 1 h) on S391 phosphorylation of endogenous CRTC3. HEK 293T cells were transfected with three different shRNA constructs against *H. sapiens* CRTC3 (C3 no 1-3; neg. = shRNA negative control). After 48 h cells were treated for 1 h with TPA (200 nM),

## Transparent Methods

Sections of the methods were previously described and are reprinted here, partly verbatim, for reference (Sonntag et al., 2017).

### Small molecules

Small molecules were solubilized in DMSO (ACS, Sigma-Aldrich) at the indicated concentrations and stored until usage at -80 °C (long term storage) or -20 °C (working dilution): 2 mM Carfilzomib (PR-171; Selleck Chemicals), 200 μM Cyclosporin A (cyclosporin; Sigma-Aldrich), 100 μM Dinaciclib (SCH727965; Selleck Chemicals), 20 mM Forskolin (Sigma-Aldrich), 20 mM Longdaysin (Sigma-Aldrich), 200 μg/ml nocodazole (Cell Signaling Technology), 1 mM Palbociclib (PD-0332991; freshly prepared in ddH<sub>2</sub>O; Selleck Chemicals), 20 mM Roscovitine (Seliciclib, CYC202; Selleck Chemicals), 100 μM SCH772984 (Selleck Chemicals), 400 μM TPA (Cell Signaling Technology).

### Antibodies

The antibodies used in this study were purchased from Abcam (PPP2R1A), Covance (GFP), EMD Millipore ( $\alpha$ -tubulin), Santa Cruz Biotechnology (14-3-3  $\epsilon$ , 14-3-3  $\zeta$ ), Sigma-Aldrich (FLAG M2), and Cell Signaling Technology (14-3-3 [pan], Calcineurin A [CaN; pan], P-Cdc2 Y15, P-CREB S133, CRT3C3 *H. sapiens* AA139 [#2720], P-CRTC2 S171, P-NPM S4, P-NPM T199, P-p44/42 MAPK [Erk1/2] T202/Y204, PPP2CA, PPP2R1A, PPP2R2A). The P-CRTC3 S273 antiserum was previously described (Sonntag et al., 2017).

See antiserum production for the rabbit P-CRTC3 S391 (PBL #7408), the rabbit hCRTC3(414-432) (PBL #7019), and the rabbit mCRTC2(454-477) (PBL #6896) antisera.

### Antiserum production

#### *Animal Care*

All animal procedures were approved by the Institutional Animal Care and Use Committee of the Salk Institute

and were conducted in accordance with the PHS Policy on Humane Care and Use of Laboratory Animals (PHS Policy, 2015), the U.S. Government Principles for Utilization and Care of Vertebrate Animals Used in Testing, Research and Training, the NRC Guide for Care and Use of Laboratory Animals (8th edition) and the USDA Animal Welfare Act and Regulations. All animals were housed in an AAALAC accredited facility in a climate controlled environment (65-72 degrees Fahrenheit, 30-70% humidity) under 12-hour light/12-hour dark cycles. Upon arrival, animals were physically examined by veterinary staff for good health and acclimated for at least two weeks prior to initiation of antiserum production. Each animal was monitored daily by the veterinary staff for signs of complications and weighed every two weeks. Routine physical exams were also performed by the veterinarian quarterly on all rabbits.

For production of each antiserum (P-CRTC3 S391, mCRTC2(454-477) and hCRTC3(414-432)), three 10 to 12-week old, female New Zealand white rabbits, weighing 3.0 to 3.2 kg at beginning of the study, were procured from Irish Farms (I.F.P.S. Inc., Norco, California, USA). Rabbits were provided with ad libitum feed (5326 Lab Diet High Fiber), micro-filtered water and weekly fruits, vegetables and alfalfa hay for enrichment.

#### *Preparation of Antigens*

Synthetic peptides were synthesized in house or by RS Synthesis (Louisville, KY), HPLC purified to >95%, and amino acid sequenced verified by mass spectrometry. Peptides were covalently attached to large carrier proteins for use as immunogens. Cys<sup>383</sup>,pSer<sup>391</sup> mCRTC3(383-395)-NH<sub>2</sub>, and Cys<sup>414</sup> hCRTC3(414-432) were conjugated to maleimide activated Keyhole Limpet Hemocyanin (KLH) per manufacturer's instructions (Thermo Fisher Scientific). mCRTC2(454-477) was conjugated to bovine thyroglobulins via glutaraldehyde, 1% final, using reagents purchased from Sigma-Aldrich.

Specific peptides used to generate antisera are as follows:

Cys<sup>383</sup>,pSer<sup>391</sup> mouse CRTC3(383-395)-NH<sub>2</sub>, CRRRQPPV(pS)PLTL-NH<sub>2</sub>;

mouse CRTC2(454-477), KQFSPTMSPTLSSITQGVPLDTSK; and

Cys<sup>414</sup> human CRTC3(414-432), CLAPYPTSQMVSSDRSLS.

### *Injection and Bleeding of Animals*

The antigen was delivered to host animals using multiple intradermal injections of peptide-KLH conjugate in Complete Freund's Adjuvant (initial inoculation) or incomplete Freund's adjuvant (booster inoculations) every three weeks. Rabbits were bled, <10% total blood volume, one week following booster injections and bleeds screened for titer and specificity. Rabbits were administered 1-2 mg/kg Acepromazine IM prior to injections of antigen or blood withdrawal. At the termination of study, rabbits were exsanguinated under anesthesia (ketamine 50 mg/kg and acepromazine 1 mg/kg, IM) and euthanized with an overdose of pentobarbital sodium and phenytoin sodium (1 ml/4.5 kg of body weight IC to effect). After blood was collected death of animals was confirmed. All animal procedures were conducted by experienced veterinary technicians, under the supervision of Salk Institute veterinarians.

### *Characterization and purification of antisera*

Each bleed from each animal was tested at multiple doses for the ability to recognize the synthetic peptide antigen; bleeds with highest titers were further analyzed by Western blot for the ability to recognize the full-length endogenous protein and to check for cross-reactivity with other proteins. Antisera with the best characteristics of titer against the synthetic peptide antigen, ability to recognize the endogenous protein, and specificity were affinity purified and used for all studies. Rabbit PBL #7408 anti P-CRTC3 S391, rabbit PBL #6896 anti-CRTC2, rabbit PBL #7019 anti-hCRTC3 were purified using Cys<sup>383</sup>,pSer<sup>391</sup>mCRTC3(383-395)-NH<sub>2</sub>, or mCRTC2(454-477), or Cys<sup>414</sup> hCRTC3(414-432), respectively, covalently attached to Sulfolink agarose (Thermo Fisher Scientific) for cysteine containing CRTC3 peptides or to Affi-Gel 10 (BioRad) for the CRTC2 peptide with N-terminal lysine. Coupling of peptides to resins was per manufacturer's instructions. To ensure that the same batch of purified antibodies could be used for this and future studies, large volumes, 20 ml rabbit sera, from bleeds with similar profiles were purified.

### **Plasmids**

For overexpression studies plasmids were used that contained the *H. sapiens* Ubiquitin C promoter (pUbC), whose activity is unaffected by cAMP signaling. The plasmids - pUbC-3xFLAG-TEVsite-His<sub>6</sub>-MCS-IRES-eGFP and pUbC-MCS-His<sub>6</sub>-TEVsite-3xFLAG-IRES-eGFP - have been described previously (MCS = multiple cloning site) (Sonntag et al., 2017).

CRTC1-3 and EGFP (Clontech) overexpression constructs were previously generated (Sonntag et al., 2017, Sonntag et al., 2018). The plasmids code for the following proteins (UniProt identifier): mCRTC1 (Q68ED7-1), mCRTC2 (Q3U182-1), and mCRTC3 (Q91X84-1) (m = *Mus musculus*).

The CRTC3 mutants were cloned by restriction enzyme digest, site-directed mutagenesis, fusion PCR (CRTC3  $\Delta$ 369-379), inverse PCR (CRTC3  $\Delta$ 330-364), and restriction-free (RF) cloning (CRTC2/3 hybrid proteins).

Fusion PCR and RF cloning were performed as previously described (Sonntag and Mootz, 2011, Sonntag, 2017).

The CRTC3 shRNA constructs were generated by cloning 5' phosphorylated double stranded hCRTC3 oligonucleotides into the *Bam*HI and *Hind*III cut pSilencer 2.1-U6 puro plasmid (Applied Biosystems):

no. 1: 5' GATCCGCTTCAGCAACTGCGCCTTTTCAAGAGAAAGGCGCAGTTGCTGAAGTTTTTTGGAAA 3'

no. 2: 5' GATCCGAAGCTCCTCTGGTCTCCATTCAAGAGATGGAGACCAGAGGAGCTTCTTTTTTTGGAAA 3'

no. 3: 5' GATCCGCACATCAAGGTTTCAGCATTCAAGAGATGCTGAAACCTTGATGTGCTTTTTTTGGAAA 3'

The empty plasmid served as negative control.

## Cell culture

HEK 293T cells were purchased from ATCC (CRL-11268) and propagated in DMEM (Gibco®, high glucose) supplemented with 10% Fetal Bovine Serum (FBS; Gemini Bio-Products) and 100 U/ml penicillin-streptomycin (Corning Inc.). Primary stromal vascular fraction (SVF) cells of brown adipose tissue (BAT) were generated from C57BL/6 wild type mice and CRTC3 knockout mice (Yoon et al., 2018):

Interscapular BAT was collected and digested for 30 min in collagenase buffer (100 mM HEPES pH 7.4, 1.5 mg/ml collagenase I [Sigma C6885], 125 mM NaCl, 5 mM KCl, 1.3 mM CaCl<sub>2</sub>, 5 mM D-glucose, and 2% BSA) with gentle shaking at 37°C. After digestion and centrifugation, SVF cells were separated from floating mature adipocytes. SVF cells were filtered and incubated in RBC lysis buffer (0.017 M Tris pH 7.4; 0.16 M NH<sub>4</sub>Cl, and

0.01 M EDTA) for 10 min at room temperature. SVF cells were centrifuged, washed, plated, and ultimately propagated in DMEM supplemented with 10% FBS and 100 U/ml penicillin-streptomycin.

### **Overexpression & immunoprecipitation (IP)**

Experiments were performed in 6 well plates by reverse transfecting HEK 293T cells ( $2.5 \times 10^6$  cells) with 2  $\mu$ g plasmid DNA using Lipofectamine® 2000 (Invitrogen). 48 h post transfection cells were collected in PBS and resuspended in lysis buffer (50 mM Tris, 150 mM NaCl, 10% glycerol, 1% Igepal [Sigma-Aldrich], 1 mM DTT, EDTA-free cOmplete™ Protease Inhibitor Cocktail [Roche], Phosphatase Inhibitor Cocktail 2 and 3 [Sigma-Aldrich], 1  $\mu$ M Carfilzomib; pH 8.0). The supernatant (= cell lysate) was either used in IP experiments or directly mixed with SDS-PAGE loading buffer. In all IP experiments, cells were pre-treated for 1 h with 1  $\mu$ M Carfilzomib prior to cell lysis. Cell lysates were incubated with anti-FLAG® M2 magnetic beads and 3xFLAG peptide (100  $\mu$ g/ml final) was used to elute bound proteins (both Sigma-Aldrich).

### **Immunoprecipitation & mass spectrometry (IP-MS)**

The IP-MS protocol and data analysis of N- and C-terminally FLAG-tagged CRTC1-3 has been previously described (Sonntag et al., 2017).

### **Immunoprecipitation of endogenous CRTC3**

Immunoprecipitation was performed from 4 x 100 mm dishes of HEK 293T cells ( $1.5 \times 10^7$  cells). 48 h post seeding cells were treated for 2 h with 200 nM SCH772984 as well as 1 h with 1  $\mu$ M Carfilzomib and 200 nM TPA. Cell lysis was performed as described in the IP protocol. HEK 293T lysate was incubated with CRTC3 rabbit hCRTC3(414-432) (PBL #7019) antiserum immobilized on Protein A magnetic beads (Dynabeads®, Life Technologies) and washed three times with lysis buffer. Bound CRTC3 protein was eluted using a CRTC3 peptide (Tyr<sup>414</sup> 415-432: YLAPYPTSQMVSSDRSQLS) resuspended in lysis buffer (100  $\mu$ g/ml final).

### **Immunofluorescence**

HEK 293T cells ( $0.75 \times 10^6$  cells) were plated in Poly-D-Lysine coated glass bottom dishes (MatTek Corporation) and under certain conditions reverse transfected with Lipofectamine® 2000 (Invitrogen) using 1 µg of mCRTC3 plasmid DNA (pUbC-3xFLAG backbone). 24 h post seeding/transfection, cells were either directly fixed with 4% paraformaldehyde or treated for 30 min with DMSO (0.05 % final), 10 µM Forskolin, 200 nM TPA prior to fixation. After incubation with primary antibodies (FLAG M2, PPP2R1A #2041, hCRTC3(414-432) PBL #7019), microscopy samples were incubated with secondary antibodies conjugated with Alexa Fluor® - 568 (goat anti-mouse / goat anti-rabbit) or in case of FLAG/PPP2R1A co-staining Alexa Fluor® - 568 and - 647 (568 - goat anti-rabbit & 647 - goat anti-mouse) (Life Technologies). Counterstaining with DAPI (Cayman Chemical Company) was performed before image acquisition (LSM 710; Carl Zeiss).

### **Luciferase reporter assays**

Assays were performed in 96 well plates by reverse transfecting HEK 293T cells (100,000 cells). For each well 80 ng of DNA was used: 10 ng of EVX-Luc reporter plasmid (2x CRE half-sites, firefly luciferase) (Sonntag et al., 2017), 10 ng of FLAG-tagged CRTC1-3 plasmids, 60 ng of empty pUbC plasmid. 24 h post transfection 10 µM Fsk or 200 nM TPA were added and cells further incubated for 4 h (Fsk) or 5 h (TPA). Under all circumstances, DMSO served as the control treatment (each well 1% DMSO final). Next, 10 µl of Bright-Glo™ (Promega) was added per well and luciferase activity measured in a GloMax® multi microplate reader (Promega).

### **Gene expression analysis**

CRTC3 WT and KO SVF cells were propagated to 60-80% confluency before (co-)treatment with 200 nM SCH772984 and DMSO (0.1 % final) for 4h and/or 10 µM Forskolin for 1h. Subsequently, cells were lysed in TRIzol® (Thermo Fisher Scientific) and RNAs extracted. cDNA was synthesized from 500 ng input RNA using First Strand cDNA synthesis kit (Roche) and quantified on a LightCycler® 480 II (Roche).

Primers used in quantitative real-time PCR (qPCR) experiments:

*RPL32*:

FP 5' TCTGGTGAAGCCCAAGATCG 3'; RP 5' CTCTGGGTTTCCGCCAGTT 3'

*NR4A1*:

FP 5' CTCTGGTTCCTGGACGTTA 3'; RP 5' AGTACCAGGCCTGAGCAGAA 3'

*RGS2*:

FP 5' AACGGCCCCAAGGTCGAGGA 3'; RP 5' CGCTTCCTCAGGAGAAGGCTT 3'

### **PP2A activity assay**

Experiments were performed in 6 well plates by reverse transfecting HEK 293T cells ( $2.5 \times 10^6$  cells) with 2  $\mu$ g plasmid DNA using Lipofectamine® 2000 (Invitrogen). 48 h post transfection cells were treated for 1 h with 1  $\mu$ M Carfilzomib, collected in PBS, and resuspended in lysis buffer (50 mM Tris, 150 mM NaCl, 10% glycerol, 1% Igepal [Sigma-Aldrich], 1 mM DTT, EDTA-free cOmplete™ Protease Inhibitor Cocktail [Roche], 1  $\mu$ M Carfilzomib; pH 8.0). The supernatant (= cell lysate) was either used in the PP2A activity assay or directly mixed with SDS-PAGE loading buffer. PP2A catalytic subunit (PPP2CA) was immunoprecipitated from cell lysates according to manufacturer's instructions (PP2A Immunoprecipitation Phosphatase Assay Kit, Upstate). Phosphate release from 0.75 mM threonine phosphopeptide (KRpTIRR) was detected by Malachite Green and measured in a Synergy™ H1 microplate reader (BioTek Instruments).

### **Cell proliferation assay**

Experiments were performed in 96 well plates by reverse transfecting HEK 293T cells (100,000 cells). In each well 80 ng of GFP or CRT3 plasmid DNA was used. Effects on HEK 293T proliferation were measured using the BrdU Cell Proliferation ELISA Kit (Abcam) according to manufacturer's instructions in a Synergy™ H1 microplate reader (BioTek Instruments). BrdU treatment occurred either for 22 h (5 h post transfection) or for 4 h (23 h post transfection) prior to the colorimetric assay 27 h post transfection.

## Sequence alignment

Amino acid sequences were aligned using MegAlign and Clustal W method (DNASTAR v7).

## Statistical analysis

Data are either presented as the mean  $\pm$  SEM. or  $\pm$  SD. One-way ANOVA was used for qPCR and CRE reporter data analysis. Statistical analyses were performed using either Microsoft Excel (Microsoft Corporation) or PRISM (GraphPad). Graphical presentations were generated using PRISM (GraphPad) and SigmaPlot (Systat Software Inc.).

## References

- BEAUSOLEIL, S. A., VILLEN, J., GERBER, S. A., RUSH, J. & GYGI, S. P. 2006. A probability-based approach for high-throughput protein phosphorylation analysis and site localization. *Nat Biotechnol*, 24, 1285-92.
- HIROTA, T., LEE, J. W., LEWIS, W. G., ZHANG, E. E., BRETON, G., LIU, X., GARCIA, M., PETERS, E. C., ETCHEGARAY, J. P., TRAVER, D., SCHULTZ, P. G. & KAY, S. A. 2010. High-throughput chemical screen identifies a novel potent modulator of cellular circadian rhythms and reveals CK1alpha as a clock regulatory kinase. *PLoS Biol*, 8, e1000559.
- MORRIS, E. J., JHA, S., RESTAINO, C. R., DAYANANTH, P., ZHU, H., COOPER, A., CARR, D., DENG, Y., JIN, W., BLACK, S., LONG, B., LIU, J., DINUNZIO, E., WINDSOR, W., ZHANG, R., ZHAO, S., ANGAGAW, M. H., PINHEIRO, E. M., DESAI, J., XIAO, L., SHIPPS, G., HRUZA, A., WANG, J., KELLY, J., PALIWAL, S., GAO, X., BABU, B. S., ZHU, L., DAUBLAIN, P., ZHANG, L., LUTTERBACH, B. A., PELLETIER, M. R., PHILIPPAR, U., SILIPHAIVANH, P., WITTER, D., KIRSCHMEIER, P., BISHOP, W. R., HICKLIN, D., GILLILAND, D. G., JAYARAMAN, L., ZAWEL, L., FAWELL, S. & SAMATAR, A. A. 2013. Discovery of a novel ERK inhibitor with activity in models of acquired resistance to BRAF and MEK inhibitors. *Cancer Discov*, 3, 742-50.
- SONNTAG, T. 2017. A Cassette Approach for the Identification of Intein Insertion Sites. *Methods Mol Biol*, 1495, 239-258.
- SONNTAG, T. & MOOTZ, H. D. 2011. An intein-cassette integration approach used for the generation of a split TEV protease activated by conditional protein splicing. *Mol Biosyst*, 7, 2031-9.
- SONNTAG, T., MORESCO, J. J., VAUGHAN, J. M., MATSUMURA, S., YATES, J. R., 3RD & MONTMINY, M. 2017. Analysis of a cAMP regulated coactivator family reveals an alternative phosphorylation motif for AMPK family members. *PLoS One*, 12, e0173013.
- SONNTAG, T., VAUGHAN, J. M. & MONTMINY, M. 2018. 14-3-3 proteins mediate inhibitory effects of cAMP on salt-inducible kinases (SIKs). *FEBS J*, 285, 467-480.
- YOON, Y. S., TSAI, W. W., VAN DE VELDE, S., CHEN, Z., LEE, K. F., MORGAN, D. A., RAHMOUNI, K., MATSUMURA, S., WIATER, E., SONG, Y. & MONTMINY, M. 2018. cAMP-inducible coactivator CRT3 attenuates brown adipose tissue thermogenesis. *Proc Natl Acad Sci U S A*.